Calculation of Wave Characteristics in Bubbly Two-Phase Flows

by

Tak-Yiu Wong

Report No. E200.6

In Partial Fulfillment of the Requirements

for the Engineer Degree

Division of Engineering and Applied Science
California Institute of Technology

October 1982

ACKNOWLEDGEMENT

I wish to express my deepest appreciation to Professor Christopher E. Brennen for his patient guidance and support throughout this research. His advice contributed greatly to this thesis. I also wish to thank Professor R. H. Sabersky for his understanding and encouragement which were very helpful during difficult times.

This research was sponsored by the National Science Foundation under Grant No. Eng. 76-11225 and by NASA under Grant No. NAS 8-29313. The generosity of their contribution is gratefully acknowledged.

Finally, I dedicate this thesis to my parents who have given me so much in supporting me through my education, and to my wife Wai-Pak who has always stood by my side at any time.

ABSTRACT

Kinematic and dynamic wave characteristics in bubbly two-phase flows are investigated. Using the same set of basic equations, kinematic and dynamic wave characteristics in a one-dimensional flow system were simultaneously obtained. A simple linear model was used so that the response of the flow to oscillatory perturbations of frequency Ω was studied. Explicit asymptotic solutions for the wave speeds and attenuations in various relative velocity and frequency regimes were obtained. Numerical analyses were carried out to investigate intermediate or transitional values of the parameters. The regimes of validity for a number of conventional wave propagation models (drift-flux model and acoustic wave analysis) were explored by using the present results. It was observed that for most engineering bubbly two-phase flows of concern, the inertial effects, which are commonly neglected in many existing models, should be included for better accuracy in prediction of wave characteristics.

TABLE OF CONTENTS

TABLE OF CONTENTS (continued)

LIST OF FIGURES

LIST OF FIGURES (continued)

LIST OF TABLES

NOMENCLATURE

C_o Acoustic velocity in stationary bubbly two-phase mixture = $\sqrt{kP_o/\alpha_o(1 - \alpha_o)\rho_{Lo}}$

C_D Drag coefficient

C Wave propagation speed

d Gas to liquid density ratio

G Relative velocity parameter = $\frac{V_{Go} - V_{Lo}}{C_o}$

G* Relative velocity between phases to liquid velocity ratio = $(V_{Go} - V_{Lo})/V_{Lo} = G/M$

g Gravity

j $\sqrt{-1}$

k Polytropic thermal constant

M Mach number of liquid = $\frac{V_{Lo}}{C_o}$

n Number of bubble per unit volume

P Pressure

R Bubble radius

Re Relative motion Reynolds number = $\frac{(V_{Go} - V_{Lo})R_o}{\nu_L}$

s Location

t Time

V_G Gas bubble velocity

V_L Liquid velocity

X Wave characteristic parameter = $(\frac{\Omega}{j\eta V_{Lo}} - 1)\frac{V_{Lo}}{C_o}$

α Void fraction

ε Perturbation terms

NOMENCLATURE (continued)

η Wave number

λ Wave-length

ν_L Liquid viscosity

ρ_G Gas density

ρ_L Liquid density

τ Bubble volume

Ω Oscillatory frequency

Ω^* Nondimensional frequency at low relative motion Reynolds number = $\frac{\Omega R_o^2}{\nu_L}$

Ω_c Nondimensional frequency at high relative motion Reynolds number = $\frac{\Omega R_o}{C_o}$

Subscripts:

G Gas

I Imaginary part of a quantity

i 1, 2, 3 or 4

L Liquid

o Mean values

R Real part of a quantity

Operators:

$$\frac{D_G}{D_G t} = \frac{\partial}{\partial t} + V_G \frac{\partial}{\partial s}$$

$$\frac{D_L}{D_L t} = \frac{\partial}{\partial t} + V_L \frac{\partial}{\partial s}$$

I. INTRODUCTION

Oscillatory behavior is commonly encountered in two-phase flow systems such as boiling-water reactors, steam generators, chemical-process reboilers, cryogenic systems, etc. Continuous oscillatory propagation phenomena can occur due to two basic types of waves in multi-phase flows, namely, kinematic waves and dynamic waves.

A kinematic wave (also known as a continuity wave) is a quasi-steady-state phenomenon and occurs whenever there is a relationship between flow rate and concentration of flow substances. One steady-state value simply propagates into another and the dynamic effects of inertia or momentum are negligible. The idea of kinematic waves was first introduced by Lighthill and Whitham [8, 9] and Kinch [10]. It has been extensively used to describe the propagation speed of the void fraction in a two-phase flow regime by Zuber [11], Wallis [12] and others. On the other hand, the existence of dynamic waves depends on forces which will accelerate the material through the wave as a result of a concentration gradient. Analyses of dynamic wave characteristics can be found in papers by Gouse and Evans [13] and by Moody [14].

Flow oscillation is dangerous in two-phase flow systems. Sustained flow oscillations may trigger numerous forms of flow instability as described and classified by Bouré [15] and Yadigaroglu [16]. These flow instabilities lead to change in local flow regimes and may cause problems such as boiling crisis (burn-out and dry-out) etc. [6].

In this paper, dynamic and kinematic wave characteristics are simultaneously evaluated from a general model for bubbly two-phase flows.

The wave characteristics are studied in detail in different relative velocity and frequency regimes.

II. BASIC EQUATIONS AND ANALYSIS

The analysis which follows determines the wave propagation speeds in a one-dimensional bubbly two-phase flow system. The model used in the analysis is non-homogeneous with the two phases having different properties and different velocities. It is assumed that the system is comprised of non-condensible compressible gas bubbles in an incompressible liquid.

The equations of continuity governing plane wave propagation in the direction s are

$$\rho_L \left[\frac{\partial}{\partial t}(1 - \alpha) + \frac{\partial}{\partial s}[(1 - \alpha)V_L]\right] = 0 \tag{1}$$

$$\frac{\partial}{\partial t}(\rho_G \alpha) + \frac{\partial}{\partial s}(\rho_G \alpha V_G) = 0 \tag{2}$$

for the gas and liquid flows respectively.

In addition to zero mass transfer between phases, it is also assumed that there is no creation or destruction of bubbles in the flow. The continuity of bubble number is thus given by:

$$\frac{\partial n}{\partial t} + \frac{\partial}{\partial s}(nV_G) = 0 \tag{3}$$

Such that $\alpha = n\tau$ and $\rho_G \tau = \text{constant}$

The global momentum-equation in one-dimensional form is given by

$$\frac{\partial}{\partial t}[\rho_L(1 - \alpha)V_L + \rho_G \alpha V_L] + \frac{\partial}{\partial s}[\rho_L(1 - \alpha)V_L^2 + \rho_G \alpha V_G^2] = -\frac{\partial p}{\partial s} + [\rho_L(1 - \alpha) + \rho_G \alpha]g \tag{4}$$

Note that the frictional terms in the momentum equation have been neglected; hence, a one-dimensional uniform flow regime is assumed and the friction with any containing walls is neglected.

The equation of relative motion between a bubble and the incompressible liquid is assumed to be that derived by Symington [1]:

$$-\frac{1}{2}\tau\frac{D_G V_G}{D_G t}-\frac{1}{2}(V_L-V_G)\frac{D_G \tau}{D_G t}-\frac{3}{2}\tau\frac{D_L V_L}{D_L t}-\tau g$$

$$=\begin{cases} 6\pi\nu_L(V_L-V_G)R & (5i) \\ \frac{C_D}{2}(V_L-V_G)|V_L-V_G|\pi R^2 & (5ii) \end{cases}$$

Physically, the four terms on the left hand side of equation (5) represent the effects of added mass of spherical bubble due to bubble acceleration, force due to bubble growth, the effect of liquid acceleration and the buoyancy force respectively. These are derived from potential flow analysis. They are rather arbitrarily equated to a drag force whose form depends on whether the relative motion is in a low or high Reynolds number regime. The viscous drag expression in equation (5i) is obtained from Stoke's law for the resistance to a moving sphere. It has been observed that Stoke's law for the drag is tolerably accurate for bubbles when the relative motion Reynolds number (Re) is small compared to unity [2]. For Reynolds numbers much larger than unity, the drag coefficient (C_D) becomes quite independent of relative motion Reynolds number. For relative motion Reynolds number within the magnitude of 10^3 to 10^5, the drag coefficient becomes approximately constant at 0.5 [3]. For most engineering bubbly two-phase flows,

when relative velocity between phases is of the order of 1 ft/sec, the bubble radius is of the order of $\frac{1}{8}$ inch and dynamic viscosity of the incompressible liquid is about 10^{-6} ft^2/sec, the relative motion Reynolds number is about 10^4. Hence, a constant C_D is usually pertinent to such engineering flows.

Since equation (5) is obtained from a potential flow analysis, another viscous effect, namely, the Basset Force [3] which is a function of the entire previous history of the bubble motion has been omitted. For a bubble moving with arbitrary speed in straight line, Landau and Lifshitz [4] obtained the result that Basset force equals

$$6\rho_L R_o^2\sqrt{\nu_L \pi}\int_{t_o}^{t}(t - t')^{-\frac{1}{2}}\left(\frac{d(V_G - V_L)}{dt'}\right)dt'$$

For the typical time T_o which is equal to $\frac{1}{\Omega}$ for a sinusoidal fluctuation the Basset force is of the order of magnitude of $\rho_L R_o^2(V_{Go} - V_{Lo})\sqrt{\nu_L \Omega}$ while the steady drag forces are of the order of $\nu_L \rho_L R_o(V_{Go} - V_{Lo})$ and $\rho_L(V_{Go} - V_{Lo})^2 R_o^2$ for low and high relative motion Reynolds number respectively. Comparing the Basset force and steady drag, it can be seen that the Basset force is negligible if the frequency of fluctuation is much less than ν_L/R_o^2 for low relative motion Reynolds number and $(V_{Go} - V_{Lo})^2/\nu_L$ for high relative motion Reynolds number. For the typical engineering bubbly two phase flow systems mentioned above (high relative motion Reynolds number), the Basset force is negligible when the frequency of fluctuation is much lower than 10^5 Hz. This is much higher than the frequency range considered in most engineering problems (up to 10^3 Hz).

From equation (5), it can be seen that at low relative motion Reynolds number, the relative velocity $(V_{Go} - V_{Lo})$ is given by $\frac{2}{9}\frac{gR_o^2}{\nu_L}$ while at high relative motion Reynolds number, $(V_{Go} - V_{Lo})$ equals $(\frac{8}{3}\frac{gR_o}{C_D})^{1/2}$.

The response of the gas inside the bubble is assumed to be governed by a polytropic thermal relationship and the surface tension effects are neglected so that the gas pressure is identical to the liquid pressure. Therefore, the equation of state for compressible gas inside the bubbles is given by

$$\rho_G = (\text{constant})P^{1/k} \tag{6}$$

In order to investigate the propagation rate of infinitesimal fluctuations, a simple linear model will be constructed. The linear dynamics of the system will be studied by considering its response to oscillatory perturbations of frequency Ω. Therefore, any quantity, Q, (such as pressure, void fraction, gas density, velocity, etc.) is decomposed into

$$Q = Q_o + \text{Re}\{\tilde{Q}e^{j\Omega t}\}$$

where Q_o is the steady part and $\text{Re}\{\tilde{Q}e^{j\Omega t}\}$ is the fluctuating part of the quantity and $\tilde{Q}$ is an exponential function of position s:

$$\tilde{Q} = (\text{constant})\ \text{Exp}\ (\eta s)$$

The quantity $\eta = \eta_R + j\eta_I$ will, in general, be a complex number such that $\Omega/\eta_I = C$ is the wave propagation speed of the fluctuation and η_R is the attenuation of fluctuation.

Other quantities of flow are denoted by

$$P = P_o + \mathrm{Re}\{\tilde{P}e^{j\Omega t}\} \quad ; \quad \tilde{P} = \sum_n A_n e^{\eta_n s}$$

$$\tau = \tau_o + \mathrm{Re}\{\tilde{\tau}e^{j\Omega t}\} \quad ; \quad \tilde{\tau} = \sum_n T_n e^{\eta_n s}$$

$$R = R_o + \mathrm{Re}\{\tilde{R}e^{j\Omega t}\} \quad ; \quad \tilde{R} = \sum_n R_n e^{\eta_n s}$$

$$\alpha = \alpha_o + \mathrm{Re}\{\tilde{\alpha}e^{j\Omega t}\} \quad ; \quad \tilde{\alpha} = \sum_n D_n e^{\eta_n s}$$

$$n = n_o + \mathrm{Re}\{\tilde{n}e^{j\Omega t}\} \quad ; \quad \tilde{n} = \sum_n N_n e^{\eta_n s}$$

$$\rho_L = \rho_{Lo}$$

$$\rho_G = \rho_{Go} + \mathrm{Re}\{\tilde{\rho}_G e^{j\Omega t}\} \quad ; \quad \tilde{\rho}_G = \sum_n B_n e^{\eta_n s}$$

$$V_L = V_{Lo} + \mathrm{Re}\{\tilde{V}_L e^{j\Omega t}\} \quad ; \quad \tilde{V}_L = \sum_n V_n e^{\eta_n s}$$

$$V_G = V_{Go} + \mathrm{Re}\{\tilde{V}_G e^{j\Omega t}\} \quad ; \quad \tilde{V}_G = \sum_n U_n e^{\eta_n s}$$

The fluctuating parts of all quantities are considered to be small in order for the linear perturbation analysis to be valid. The summation functions for the fluctuating parts denote the linear superposition of multiple solutions corresponding to multiple waves obtained.

By eliminating all quantities except P and α from equation (1) to (6), the following relation is obtained:

$$\frac{\alpha_o}{kP_o} A_n = \frac{D_n}{(1 - \alpha_o)} \frac{[\gamma\eta_n^2 + \zeta\eta_n + \beta]}{[\theta\eta_n^2 + \psi\eta_n + \delta]}$$

Such that at relative motion Reynolds number small compared to unity:

$$\gamma = -\frac{1}{2}\tau_o[V_{Go}^2(1-\alpha_o) + 3V_{Lo}^2\alpha_o]$$

$$\zeta = -6\pi\nu_L R_o[V_{Lo}\alpha_o + V_{Go}(1-\alpha_o)] - j\tau_o\Omega[V_{Go}(1-\alpha_o) + 3V_{Lo}\alpha_o]$$

$$\beta = \frac{1}{2}\tau_o\Omega^2[(1-\alpha_o) + 3\alpha_o] - j6\pi\nu_L R_o\Omega[\alpha_o + (1-\alpha_o)]$$

$$\theta = \frac{1}{2}\tau_o V_{Go}[2V_{Go} - V_{Lo}] \qquad (7i)$$

$$\psi = 2\pi\nu_L R_o(4V_{Go} - V_{Lo}) - \tau_o g + j\frac{1}{2}\tau_o\Omega(3V_{Go} - V_{Lo})$$

$$\delta = -\frac{1}{2}\tau_o\Omega^2 + j6\pi\nu_L\Omega R_o$$

while at relative motion Reynolds number much larger than unity:

$$\gamma = -\frac{1}{2}\tau_o[V_{Go}^2(1-\alpha_o) + 3V_{Lo}^2\alpha_o]$$

$$\zeta = C_D\pi R_o^2(V_{Lo} - V_{Go})[V_{Lo}\alpha_o + V_{Go}(1-\alpha_o)] - j\tau_o\Omega[V_{Go}(1-\alpha_o) + 3V_{Lo}\alpha_o]$$

$$\beta = \frac{1}{2}\tau_o\Omega^2[(1-\alpha_o) + 3\alpha_o] - jC_D\pi R^2(V_{Go} - V_{Lo})\Omega[\alpha_o + (1-\alpha_o)] \qquad (7ii)$$

$$\theta = \frac{1}{2}\tau_o V_{Go}(2V_{Go} - V_{Lo})$$

$$\psi = \frac{C_D}{3}\pi R_o^2(V_{Go} - V_{Lo})(4V_{Go} - V_{Lo}) - \tau_o g + j\frac{1}{2}\tau_o\Omega(3V_{Go} - V_{Lo})$$

$$\delta = -\frac{1}{2}\tau_o\Omega^2 + jC_D\pi R_o^2\Omega(V_{Go} - V_{Lo})$$

Finally, a quartic dispersion relation is obtained for a modified wave paramater, X. This is a function of frequency and wave number obtained from a Lagrangian frame of reference travelling with the steady velocity of liquid such that

$$X = \left(\frac{\Omega}{jnV_{Lo}} - 1\right)\frac{V_{Lo}}{C_o} \qquad (8)$$

The quantity C_o is the acoustic velocity in the stationary two-phase mixture and is equal to $\sqrt{kP_o/\alpha_o(1 - \alpha_o)\rho_{Lo}}$ [5], and

$$\frac{\Omega}{V_{Lo}\eta_I} = \frac{C}{V_{Lo}} = \frac{(\frac{M}{G} + \frac{X_R}{G})^2 + (\frac{X_I}{G})^2}{\frac{M}{G}(\frac{M}{G} + \frac{X_R}{G})} \tag{9}$$

$$\frac{\eta_R V_{Lo}}{\Omega} = \frac{-(\frac{M}{G})(\frac{X_I}{G})}{(\frac{M}{G} + \frac{X_R}{G})^2 + (\frac{X_I}{G})^2} \tag{10}$$

where $G = (V_{Go} - V_{Lo})/C_o$ and $M = V_{Lo}/C_o$. The quartic dispersion relations for X then becomes

(a) At low relative motion Reynolds number

$$(\frac{X}{G})^4\left\{1 - \frac{9j}{\Omega^*}\right\} +$$

$$(\frac{X}{G})^3\left\{-3 + \frac{9j}{\Omega^*}[\frac{5}{6} - \frac{M}{G}] + (\frac{9}{\Omega^*})^2\frac{1}{2}\right\} +$$

$$(\frac{X}{G})^2\left\{2 - \frac{1 + 2\alpha_o}{G^2} + \frac{9j}{\Omega^*}[\frac{1}{G^2} - \frac{3}{2} + \frac{5}{6}\frac{M}{G}] + (\frac{9}{\Omega^*})^2[-\frac{1}{6} + \frac{M}{G}]\right\} + \tag{11}$$

$$(\frac{X}{G})^1\left\{2\frac{1 - \alpha_o}{G^2} + \frac{9j}{\Omega^*}[1 - \frac{1 - \alpha_o}{G^2} - \frac{3}{2}\frac{M}{G} + \frac{M}{G^3}] + (\frac{9}{\Omega^*})^2[-\frac{1}{3}\frac{M}{G} + \frac{1}{2}\frac{M^2}{G^2}]\right\} +$$

$$(\frac{X}{G})^0\left\{-\frac{1 - \alpha_o}{G^2} + \frac{9j}{\Omega^*}[\frac{M}{G} - \frac{M}{G^3}(1 - \alpha_o)] + (\frac{9}{\Omega^*})^2[-\frac{1}{6}\frac{M^2}{G^2}]\right\} = 0$$

(b) At high relative motion Reynolds number

$$\left(\frac{X}{G}\right)^4\left\{1 - j\,\frac{3C_DG}{2\Omega_c}\right\} +$$

$$\left(\frac{X}{G}\right)^3\left\{-3 + j\,\frac{3C_DG}{2\Omega_c}\left[\frac{13}{12} - \frac{M}{G}\right] + \left(\frac{3C_DG}{2\Omega_c}\right)^2\frac{1}{4}\right\} + \qquad (12)$$

$$\left(\frac{X}{G}\right)^2\left\{2 - \frac{1 + 2\alpha_o}{G^2} + j\,\frac{3C_DG}{2\Omega_c}\left[\frac{1}{G^2} - \frac{3}{4} + \frac{13}{12}\frac{M}{G}\right] + \left(\frac{3C_DG}{2\Omega_c}\right)^2\left[-\frac{5}{24} + \frac{1}{2}\frac{M}{G}\right]\right\} +$$

$$\left(\frac{X}{G}\right)^1\left\{2\,\frac{1 - \alpha_o}{G^2} + j\,\frac{3C_DG}{2\Omega_c}\left[\frac{1}{2} - \frac{1 - \alpha_o}{G^2} - \frac{3}{4}\frac{M}{G} + \frac{M}{G^3}\right] + \left(\frac{3C_DG}{2\Omega_c}\right)^2\left[-\frac{5}{12}\frac{M}{G} + \frac{1}{4}\frac{M^2}{G^2}\right]\right\} +$$

$$\left(\frac{X}{G}\right)^0\left\{-\frac{1 - \alpha_o}{G^2} + j\,\frac{3C_DG}{2\Omega_c}\left[\frac{1}{2}\frac{M}{G} - \frac{M}{G^3}(1 - \alpha_o)\right] + \left(\frac{3C_DG}{2\Omega_c}\right)^2\left[-\frac{5}{24}\frac{M^2}{G^2}\right]\right\} = 0$$

It should be noted that gas density terms are omitted from equations (11) and (12) because of the fact that the ratio of gas density to liquid density is generally so small that the ratio ρ_{Go}/ρ_{Lo} can be neglected.

Solving equations (11) and (12) will provide information on the propagation rates of fluctuations and their corresponding rates of attenuation as presented in the following section. Although the quartic equations for X are too complicated for explicit solutions, it can be observed that explicit asymptotic solutions can be obtained for various asymptotic choices of the frequency (Ω^* or Ω_c/C_DG), the relative motion parameter, $G = (V_{Go} - V_{Lo})/C_o$ and Mach number, $M = V_{Lo}/C_o$.

III. PRESENTATION OF ANALYTICAL RESULTS

In the previous section, it was shown that equations (8) and (9) provide various asymptotic solutions for X depending on the magnitudes of the frequency parameter Ω^* or $\Omega_c/C_D G$. Hence, the wave speeds may be different in different relative motion Reynolds number and oscillatory frequency regimes. In addition, the wave speeds are strong functions of the relative velocity between the phases and the material velocity (i.e., G and M). In the following analysis, attention is focused on flow regimes for which M is of the order of one or less. But, both cases for $G << 1$ and $G >> 1$ will be investigated. Since relative velocity is generally of the order of 1 ft/sec when acoustic velocity is of the order of 10^2 ft/sec., the case, $G >> 1$, is considered highly hypothetical. It only provides the reader with a background to better understand how the wave speeds would change with relative velocity between the phases.

Examine first the low relative motion Reynolds number flow regime. The first particular case of interest is the case when gravity equals zero. Since relative velocity, $(V_{Go} - V_{Lo}) = \frac{2}{9}\frac{gR_o^2}{\nu_L}$, the relative velocity parameter G equals zero at zero gravity. Hence, equation (11) becomes

$$X^4\left\{1 - \frac{9j}{\Omega^*}\right\} + X^3\left\{-\frac{9j}{\Omega^*}M\right\} + X^2\left\{-(1 + 2\alpha_o) + \frac{9j}{\Omega^*}\right\} + X\left\{\frac{9j}{\Omega^*}\right\} = 0 \qquad (13)$$

3.1. Waves for Zero Mean Relative Velocity

3.1.1. Zero Mean Relative Velocity and High Frequency

The high frequency case refers to the frequency parameter Ω^*

much larger than unity. In the limit as Ω^* tends to infinity, the governing equation (from equation (13)) becomes

$$X^4 - X^2(1 + 2\alpha_o) = 0 \tag{14}$$

Note that the X values obtained from equation (13) are complex numbers though the lowest order terms from (14) are purely real. Therefore, by linearization method, let $X = \bar{X} + \varepsilon$, such that from equation (14), the lowest order terms are:

$$\begin{aligned} \bar{X}_{1,2} &= 0 \\ \bar{X}_{3,4} &= \pm\sqrt{1 + 2\alpha_o} \end{aligned} \tag{15}$$

And the first perturbation terms ε are obtained from linearization of equation (13) such that

$$\begin{aligned} (\bar{X})\ (\bar{X}^2 - (1 + 2\alpha_o)) + \varepsilon[3\bar{X}^2 - (1 + 2\alpha_o)] + \frac{9j}{\Omega^*}\ (\bar{X} + M)\ (1 - \bar{X}^2) + \\ \frac{9j}{\Omega^*}\ \varepsilon(1 - 3\bar{X}^2 - 2\bar{X}M) \approx 0 \end{aligned} \tag{16}$$

Since $\bar{X}_i = 0, \pm\sqrt{1 + 2\alpha_o}$ from expression (15), first term of equation (16) vanishes, hence,

$$\varepsilon_i \approx \frac{9j}{\Omega^*} \frac{(\bar{X}_i^{\,2} - 1)\ (\bar{X}_i + M)}{3\bar{X}_i^{\,2} - (1 + 2\alpha_o)} \tag{17}$$

That is

$$X_i = \bar{X}_i + \frac{9j}{\Omega^*} \frac{(\bar{X}_i^{\,2} - 1)\ (\bar{X}_i + M)}{3\bar{X}_i^{\,2} - (1 + 2\alpha_o)} \tag{18}$$

Expressions (15) and (18) are substituted into equations (9) and (10), neglecting the first order perturbation when summation of the fundamental and perturbation terms is made. Wave speeds and their corresponding attenuations can be obtained as illustrated in Table 1.

From the expressions in Table 1, it can be seen that two kinematic waves and two dynamic waves can be observed when a bubbly two phase flow system is subjected to oscillation. At zero relative velocity and high frequency, the wave speeds travel at the liquid velocity. The first kinematic wave as presented in Table 1 is of constant amplitude while the second kinematic wave is an attenuated wave. It can be shown that this wave loses half its amplitude over a distance of $(\Omega/2\pi C\eta_R)\ln(1/2)$ wave-lengths. For the typical engineering bubbly two phase flow discussed previously, the second kinematic wave will travel approximately 10^3 wave lengths before fifty percent of the wave amplitude is lost when the wave length is of the order of 10^{-2} ft. Therefore, in a small scale laboratory experimental setup, the attenuated wave should be observable. But in a large scale flow system such as a pipe-line, it would become insignificant. Unlike the kinematic waves, both of which travel downstream for all liquid velocities, one of the dynamic waves travels upstream when Mach number, M, is smaller than $\sqrt{1 + 2\alpha_o}$ and travels downstream otherwise. Both dynamic waves are attenuated waves and they would travel approximately 10^5 wave-lengths before they are attenuated by fifty percent of their amplitudes.

3.1.2. Zero Mean Relative Velocity and Low Frequency

The low frequency case refers to a frequency parameter Ω^* much less than unity, such that governing equation from equation (13) which

dominates the zero gravity flow at low frequency of oscillation is given by:

$$X^4 + MX^3 - X^2 - MX = 0 \tag{19}$$

Again, by linearization method, it can be shown that:

$$\begin{aligned} \bar{X}_1 &= 0 \\ \bar{X}_2 &= -M \\ \bar{X}_{3,4} &= \pm 1 \end{aligned} \tag{20}$$

And

$$\varepsilon_i = \frac{\Omega^* j}{9} \frac{(\bar{X}_i)\,(\bar{X}_i^2 - (1 + 2\alpha_o))}{(1 - 3\bar{X}_i^2 - 3\bar{X}_i M^2)} \qquad i = 1,2,3,4 \tag{21}$$

This linearization procedure works well for X_1, X_3 and X_4 but a problem exists in the derivation of X_2. By substituting expressions (20) and (21) into equation (9), a zero value is obtained in the denominator for expression of C_2. Therefore, a second order perturbation must be carried out to obtain a real part of X_2. Let $\varepsilon_2 = \varepsilon_{R2} + j\varepsilon_{I2}$, and substitute $\bar{X}_2 = -M$ into equation (13). It can be shown that

$$\frac{9j}{\Omega^*}\varepsilon(1 - \varepsilon^2 + 2\varepsilon M - M^2) + (\varepsilon - M)[(\varepsilon^2 - 2\varepsilon M + M^2) - (1 + 2\alpha_o)] = 0$$

Such that

$$\varepsilon_2 = j\,\frac{\Omega^*}{9} \frac{[M(1 + 2\alpha_o - M^2) + \varepsilon(-1 - 2\alpha_o + 3M^2)]}{(1 - M^2)\left[1 + \dfrac{2\varepsilon M}{(1 - M^2)}\right]} \tag{22}$$

By Taylor's Expansion, expression (22) becomes

$$\varepsilon_2 = j\,\frac{\Omega^*}{9}\,\frac{[M(1 + 2\alpha_o - M^2) - \varepsilon(1 + 2\alpha_o - 3M^2)]\,[1 - M^2 - 2\varepsilon M]}{(1 - M^2)^2}$$

Hence, the real and imaginary parts

$$\left.\begin{aligned}\varepsilon_{R2} &= -\left(\frac{\Omega^*}{9}\right)^2\left[\frac{M(1 + 2\alpha_o - M^2)\,(-M^4 + 2(1 - \alpha_o)M^2 - (1 + 2\alpha_o))}{(1 - M^2)^3}\right] \\ \varepsilon_{I2} &= \frac{\Omega^*}{9}\,\frac{M(1 + 2\alpha_o - M^2)}{(1 - M^2)}\end{aligned}\right\} \quad (23)$$

Substituting expressions (20), (21) and (23) into equations (9) and (10), the wave propagation characteristics are illustrated in Table 2.

It can be seen from the expressions presented in Table 2 that at asymptotically small Mach number, the kinematic wave characteristics at low frequency are basically identical to those in the high frequency regime. However, as the Mach number tends to unity, the second kinematic wave speed tends to zero. In the low frequency regime when the frequency is of the order of 10^{-3} Hz ($\Omega^* \sim 10^{-1}$), the attenuated kinematic wave, which has a wavelength of the order of 10^3 ft, vanishes in a distance less than one wave length ($10^{-2}\ \lambda$).

The dynamic wave characteristics at low frequency are similar to those at high frequency except for their attenuations. At low frequency, the attenuation of the dynamic waves is proportional to the square of the frequency parameter, while at high frequency attenuation is independent of frequency.

Wave #1 (kinematic wave)

$$\frac{C_1 - V_{Lo}}{V_{Lo}} = 0 \quad ; \quad \frac{\eta_{R1}}{\left(\frac{\nu_L}{V_{Lo}R_o^2}\right)} = 0$$

Wave #2 (kinematic wave)

$$\frac{C_2 - V_{Lo}}{V_{Lo}} = 0 \quad ; \quad \frac{\eta_{R2}}{\left(\frac{\nu_L}{V_{Lo}R_o^2}\right)} = -\frac{9}{1 + 2\alpha_o}$$

Wave #3 (dynamic wave)

$$\frac{C_3 - V_{Lo}}{C_o} = \sqrt{1 + 2\alpha_o} \quad ; \quad \frac{\eta_{R3}}{\left(\frac{\nu_L}{C_oR_o^2}\right)} = -\frac{9\alpha_o}{(1 + 2\alpha_o)\left(\sqrt{1 + 2\alpha_o} + M\right)}$$

Wave #4 (dynamic wave)

$$\frac{C_4 - V_{Lo}}{C_o} = -\sqrt{1 + 2\alpha_o} \quad ; \quad \frac{\eta_{R4}}{\left(\frac{\nu_L}{C_oR_o^2}\right)} = +\frac{9\alpha_o}{(1 + 2\alpha_o)\left(\sqrt{1 + 2\alpha_o} - M\right)}$$

Table 1. Waves in zero gravity; hence zero relative velocity ($G = 0$) and high frequency ($\Omega^* >> 1$).

Wave #1 (kinematic wave)

$$\frac{C_1 - V_{Lo}}{V_{Lo}} = 0 \quad ; \quad \frac{\eta_R}{\left(\frac{\nu_L}{V_{Lo}R_o^2}\right)} = 0$$

Wave #2 (kinematic wave)

$$\frac{C_2 - V_{Lo}}{V_{Lo}} = -\frac{4\alpha_o M^2}{M^4 - 2(1 - \alpha_o)M^2 + (1 + 2\alpha_o)} \quad ; \quad \frac{\eta_{R2}}{\left(\frac{\nu_L}{V_{Lo}R_o^2}\right)} = \frac{-9(1 - M^2)}{(1 + 2\alpha_o - M^2)}$$

Wave #3 (dynamic wave)

$$\frac{C_3 - V_{Lo}}{C_o} = 1 \quad ; \quad \frac{\eta_{R3}}{\left(\frac{\nu_L}{C_o R_o^2}\right)} = -\frac{\Omega^{*2}}{9}\frac{\alpha_o}{(1 + M)^3}$$

Wave #4 (dynamic wave)

$$\frac{C_4 - V_{Lo}}{C_o} = -1 \quad ; \quad \frac{\eta_{R3}}{\left(\frac{\nu_L}{C_o R_o^2}\right)} = +\frac{\Omega^{*2}}{9}\frac{\alpha_o}{(1 - M)^3}$$

Table 2. Waves in zero gravity; hence, zero relative velocity ($G = 0$) and low frequency ($\Omega^* << 1$).

3.2. Waves with Mean Relative Velocity at Low Reynolds Number

For most engineering bubbly two-phase flows, the relative velocity between the phases generally exists due to buoyancy and the relative velocity parameter is no longer equal to zero. The following analyses will investigate the effect of relative velocity between phases on the wave characteristics.

3.2.1. Waves for Small Relative Velocity ($G << 1$) and High Frequency ($\Omega^* >> 1$)

When the reduced frequency, Ω^*, is much larger than unity, equation (11) becomes

$$\left.\begin{aligned}\left(\frac{X}{G}\right)^4 + \left(\frac{X}{G}\right)^3 \left\{-3\right\} + \left(\frac{X}{G}\right)^2 \left\{2 - \frac{1 + 2\alpha_o}{G^2}\right\} + \\ \left(\frac{X}{G}\right) \left\{2\,\frac{1 - \alpha_o}{G^2}\right\} + \left\{-\frac{1 - \alpha_o}{G^2}\right\} = 0\end{aligned}\right\} \tag{24}$$

For the kinematic waves, it is expected that the parameter $\left(\frac{X}{G}\right)$ is of the order of unity. Then for the small relative velocity case ($G << 1$), the dominant terms of equation (24) yield

$$\left(\frac{X}{G}\right)^2 (1 + 2\alpha_o) - \left(\frac{X}{G}\right) \left\{2(1 - \alpha_o)\right\} + (1 - \alpha_o) = 0 \tag{25}$$

Hence

$$\frac{X_i}{G} = \frac{1 - \alpha_o}{1 + 2\alpha_o} \mp j\,\frac{\sqrt{3\alpha_o(1 - \alpha_o)}}{1 + 2\alpha_o} \quad ; \qquad i = 1,2$$

and

$$\frac{C_i - V_{Lo}}{V_{Lo}} = \frac{G}{M}(1 - \alpha_o)\left[\frac{1 + \frac{G}{M}}{(1 - \alpha_o)\frac{G}{M} + (1 + 2\alpha_o)}\right] \quad ; \quad i = 1,2 \qquad (26)$$

$$\frac{\eta_{Ri}}{\left(\frac{\nu_L}{V_{Lo}R_o^2}\right)} = (-1)^{i+1}\frac{\Omega^* \frac{G}{M}\sqrt{3\alpha_o(1 - \alpha_o)}}{(1 + 2\alpha_o) + 2\frac{G}{M}(1 - \alpha_o) + \left(\frac{G}{M}\right)^2(1 - \alpha_o)} \quad ; \quad i = 1,2 \qquad (27)$$

Expression (26) shows that as G tends to zero, C_1 and C_2 both tend to V_{Lo} and therefore these wave speeds correspond to kinematic waves. However, it should also be noted that as G tends to zero, the attenuation of the second kinematic wave, η_{R2}, presented in expression (27) is different from that presented in Table 1. It is understandable that as relative velocity between phases equals zero, the inertial effect dominates the flow. However, for non-zero relative velocity (i.e., $G \neq 0$), the drag force terms become significant so rapidly that the leading terms, X^4 and X^3 term in equation (11) becomes negligible resulting in different results for the two cases. Furthermore, when the parameter $|\frac{G}{M}|$ is of the order of unity, the expression of η_{R2} as presented in expression (27) is proportional to the frequency parameter, Ω^*. For Ω^* much larger than unity, expression (27) corresponds to a lower order term compared to that in Table 1.

The dynamic waves in this same asymptotic case ($\Omega^* >> 1$, $G << 1$) will have values of $|\frac{X}{G}|$ much larger than unity and under these conditions

$$\left|\left(\frac{X}{G}\right)^4\right| >> \left|-3\left(\frac{X}{G}\right)^3\right| >> \left|2\left(\frac{X}{G}\right)^2\right|$$

$$\left|-\frac{1+2\alpha_o}{G^2}\left(\frac{X}{G}\right)^2\right| >> \left|2\frac{1-\alpha_o}{G}\left(\frac{X}{G}\right)\right| >> \left|-\frac{1-\alpha_o}{G^2}\right|$$

and hence the dominant terms in equation (24) yield

$$\left(\frac{X}{G}\right)^4 - \left(\frac{X}{G}\right)^2\left(\frac{1+2\alpha_o}{G^2}\right) \approx 0 \qquad (28)$$

Therefore,

$$\frac{X_i}{G} = \frac{\sqrt{1+2\alpha_o}}{G} + \varepsilon_i \quad ; \quad i = 3,4$$

and linearization of equation (11) yields

$$\varepsilon_i = \frac{1+8\alpha_o}{2(1+2\alpha_o)} + \frac{9j}{\Omega^*}\left[\frac{\alpha_o(M \pm \sqrt{1+2\alpha_o})}{G(1+2\alpha_o)} + \frac{(1-16\alpha_o)(M \pm \sqrt{1+2\alpha_o})}{12(1+2\alpha_o)\sqrt{1+2\alpha_o}}\right] ; \qquad (29)$$

$$i = 3,4$$

Hence

$$\frac{C_i - V_{Lo}}{C_o} = \pm\sqrt{1+2\alpha_o} + \frac{1+8\alpha_o}{2(1+2\alpha_o)}G \quad ; \quad i = 3,4 \qquad (30)$$

$$\frac{\eta_{Ri}}{\left(\frac{\nu_L}{C_o R^2}\right)} = \frac{-9\left[\alpha_o + \frac{1-16\alpha_o}{12\sqrt{1+2\alpha_o}}G\right]}{(1+2\alpha_o)(M \pm \sqrt{1+2\alpha_o})} \quad ; \quad i = 3,4 \qquad (31)$$

A summary of the above analysis is provided in Table 3.

In this small velocity and high frequency regime ($G << 1$ and $\Omega^* >> 1$), the more interesting wave is the first kinematic wave as presented in Table 3 because it increases in amplitude. As an example of a typical low relative motion Reynolds number flow, we will use a highly viscous oil with dynamic viscosity of the order of 10^{-2} ft^2/sec, a bubble radius of the order $\frac{1}{8}$ in. and liquid velocity of the order of 1 ft/sec.

The relative velocity which is equal to $\frac{2}{9}\frac{gR_o^2}{\nu_L}$ would then be of the order of 0.1 ft/sec leading to a relative motion Reynolds number of approximately 0.1. The distance the growing kinematic wave would travel before doubling its amplitude is equivalent to approximately one wave-length for a wave-length of the order of 10^3 to 1 ft as frequency is of the order of 10^{-1} to 10^2 Hz. Therefore, a kinematic shock would be expected as the continuous kinematic wave intensifies and steepens downstream. On the other hand, the second kinematic wave which is an attenuated wave would decline at the same rate with which the first kinematic wave intensifies and would therefore disappear rapidly.

Using the same high viscous liquid/gas mixture as an example, the dynamic wave would decline to fifty percent of its amplitude in a distance equivalent to approximately 10 wave lengths for a wavelength of the order of 1 ft.

3.2.2. Waves for Large Relative Velocity ($G >> 1$) and High Frequency ($\Omega^* >> 1$)

In this asymptotic limit both G and Ω^* are much larger than

unity and the dominant terms in equation (24) yield

$$\left(\frac{X}{G}\right)^4 + \left(\frac{X}{G}\right)^3\{-3\} + \left(\frac{X}{G}\right)\{2\} = 0 \tag{32}$$

Such that:

$$\left.\begin{aligned} X_1 &= G + \varepsilon_1 \\ X_2 &= 2G + \varepsilon_2 \\ X_{3,4} &= 0 + \varepsilon_{3,4} \end{aligned}\right\} \tag{33}$$

Linearization of equation (11) yields

$$\left.\begin{aligned} \varepsilon_1 &= -\frac{3\alpha_o}{G} - \frac{9j}{\Omega^*}\left[\frac{4}{6} + \frac{4}{6}\frac{M}{G}\right]G \\ \varepsilon_2 &= \frac{1 + 11\alpha_o}{4G} + \frac{9j}{\Omega^*}\left[\frac{20}{6} + \frac{10}{6}\frac{M}{G}\right]G \end{aligned}\right\} \tag{34}$$

However, for $\bar{X}_{3,4} = 0$, $\varepsilon_{3,4}$ become the fundamental terms. Taking $\varepsilon_{3,4}^2$ terms into consideration in the linearization process yields

$$\varepsilon_{3,4} = \pm\frac{1}{G^2}\sqrt{\frac{1 - \alpha_o}{2}} - \frac{9j}{4\Omega^*}\left[1 + \sqrt{\frac{2}{1 - \alpha_o}}\,M\right] \tag{35}$$

Substitution of expressions (34) and (35) into equations (9) and (10) provides the wave characteristics for high relative velocity and high frequency as presented in Table 4.

It can be seen that one kinematic wave and one dynamic wave intensify as they propagate downstream. This relative motion and frequency regime is the only case when both kinematic and dynamic shocks can be expected to develop.

Wave #1 (kinematic wave)

$$\frac{C_1 - V_{Lo}}{V_{Lo}} = \frac{G}{M}(1 - \alpha_o)\left[\frac{G + M}{G(1 - \alpha_o) + M(1 + 2\alpha_o)}\right]$$

$$\frac{\eta_{R1}}{\left(\frac{\nu_L}{V_{Lo}R_o^2}\right)} = \frac{\Omega^* MG\sqrt{3\alpha_o(1 - \alpha_o)}}{M^2(1 - 2\alpha_o) + 2MG(1 - \alpha_o) + G^2(1 - \alpha_o)}$$

Wave #2 (kinematic wave)

$$\frac{C_2 - V_{Lo}}{V_{Lo}} = \frac{G}{M}(1 - \alpha_o)\ \frac{G + M}{G(1 - \alpha_o) + M(1 + 2\alpha_o)}$$

$$\frac{\eta_{R2}}{\left(\frac{\nu_L}{V_{Lo}R_o^2}\right)} = \frac{-\Omega^* MG\sqrt{3\alpha_o(1 - \alpha_o)}}{M^2(1 + 2\alpha_o) + 2MG(1 - \alpha_o) + G^2(1 - \alpha_o)}$$

Wave #3 (dynamic wave)

$$\frac{C_3 - V_{Lo}}{C_o} = \sqrt{1 + 2\alpha_o} + \frac{1 + 8\alpha_o}{2(1 + 2\alpha_o)}G$$

$$\frac{\eta_{R3}}{\left(\frac{\nu_L}{C_o R_o^2}\right)} = \frac{-9\left[\alpha_o + \frac{1}{12}\frac{1 - 16\alpha_o}{\sqrt{1 + 2\alpha_o}}G\right]}{(1 + 2\alpha_o)(\sqrt{1 + 2\alpha_o} + M)}$$

Wave #4 (dynamic wave)

$$\frac{C_4 - V_{Lo}}{C_o} = -\sqrt{1 + 2\alpha_o} + \frac{1 + 8\alpha_o}{2(1 + 2\alpha_o)}G$$

$$\frac{\eta_{R4}}{\left(\frac{\nu_L}{C_o R_o^2}\right)} = \frac{+9\left[\alpha_o + \frac{1}{12}\frac{1 - 16\alpha_o}{\sqrt{1 + 2\alpha_o}}G\right]}{(1 + 2\alpha_o)(\sqrt{1 + 2\alpha_o} - M)}$$

Table 3. Waves at small relative velocity ($G \ll 1$) and high frequency ($\Omega^* \gg 1$) for the low Reynolds number flow regime.

Wave #1 (kinematic wave)

$$\frac{C_1 - V_{Lo}}{V_{Lo}} = \frac{G}{M}$$

$$\frac{\eta_{RI}}{\left(\frac{\nu_L}{V_{Lo}R_o^2}\right)} = \frac{6M}{(M + G)}$$

Wave #2 (kinematic wave)

$$\frac{C_2 - V_{Lo}}{V_{Lo}} = \frac{2G}{M}$$

$$\frac{\eta_{RI}}{\left(\frac{\nu_L}{V_{Lo}R_o^2}\right)} = -\frac{15M}{(M + 2G)}$$

Wave #3 (dynamic wave)

$$\frac{C_3 - V_{Lo}}{C_o} = \sqrt{\frac{1 - \alpha_o}{2}}$$

$$\frac{\eta_{R3}}{\left(\frac{\nu_L}{C_oR_o^2}\right)} = \frac{9G}{\sqrt{2(1 - \alpha_o)}\left(\sqrt{2(1 - \alpha_o)} + 2M\right)}$$

Wave #4 (dynamic wave)

$$\frac{C_4 - V_{Lo}}{C_o} = -\sqrt{\frac{1 - \alpha_o}{2}}$$

$$\frac{\eta_{R4}}{\left(\frac{\nu_L}{C_oR_o^2}\right)} = \frac{+9G}{\sqrt{2(1 - \alpha_o)}\left(\sqrt{2(1 - \alpha_o)} - 2M\right)}$$

Table 4. Waves at high relative velocity ($G >> 1$) and high frequency ($\Omega^* >> 1$) for the low Reynolds number flow regime.

3.2.3. Waves for Small Relative Velocity and Low Frequency

$G << \Omega^* << 1$

For flow corresponding to low frequency of oscillation such that the reduced frequency Ω^* is much less than unity, the dominant terms in equation (11) yield

$$\left(\frac{X}{G} + \frac{M}{G}\right)\left\{-\left(\frac{X}{G}\right)^3 + \frac{5}{6}\left(\frac{X}{G}\right)^2 + \left(\frac{1}{G^2} - \frac{3}{2}\right)\left(\frac{X}{G}\right) + \left(1 - \frac{1 - \alpha_o}{G^2}\right)\right.$$

$$\left. - \frac{9j}{\Omega^*}\left(\frac{X}{G} + \frac{M}{G}\right)\left[\frac{1}{2}\left(\frac{X}{G}\right) - \frac{1}{6}\right]\right\} \approx 0 \tag{36}$$

In the domain in which the relative velocity is so small that G is much less than Ω^*, equation (36) becomes

$$\left(\frac{X}{G} + \frac{M}{G}\right)\left[\frac{X}{G} - (1 - \alpha_o)\right] = 0 \tag{37}$$

Hence

$$\left.\begin{aligned} \frac{X_1}{G} &= (1 - \alpha_o) + \varepsilon_1 \\ \frac{X_2}{G} &= -\frac{M}{G} + \varepsilon_2 \end{aligned}\right\} \tag{38}$$

where

$$\varepsilon_1 = + \frac{9j}{\Omega^*}\left[\frac{1}{2}(1 - \alpha_o) - \frac{1}{6}\right]\left[1 - \alpha_o + \frac{M}{G}\right] G^2 \tag{39}$$

$$\varepsilon_2 = -\left(\frac{\Omega^*}{9}\right)^2 AB - j\,\frac{\Omega^*}{9}\,A$$

$$A = \frac{[M^2(M+G)(M+2G) - (1-\alpha_o)(M+G)^2 - 3\alpha_o M^2]}{[-M^3 - \frac{5}{6}GM^2 + M + G(1-\alpha_o)]} \tag{40}$$

$$B = \frac{\left\{-(4M+5G)(G+M)M + 2(1-\alpha_o)(M+G) + 6\alpha_o M\right\} x \left\{-M^3 - \frac{5}{6}GM^2 + M + G(1-\alpha_o)\right\} - \left\{3M^2 - 1\right\} x \left\{M^2(M+G)(M+2G) - (1-\alpha_o)(M+G)^2 - 3\alpha_o M^2\right\}}{\left\{-M^3 - \frac{5}{6}GM^2 + M + G(1-\alpha_o)\right\}^2}$$

The wave information obtained is summarized in Table 5. Note that the waves obtained from the analysis above are kinematic waves only. The dynamic wave information is lost due to the loss of leading terms of equation (36) in the linearization process. The same situation is true for the following analysis for the case where $\Omega^* \ll 1$ and $\Omega^* \ll G$.

3.2.4. Waves for Relative Velocity and Low Frequency Such That $\Omega^* \ll 1$ and $\Omega^* \ll G$

For waves with low frequency such that $\Omega^* \ll 1$ and a relative velocity parameter larger than the reduced frequency ($\Omega^* \ll G$), the dominant terms of equation (36) yield

$$\left(\frac{X}{G} + \frac{M}{G}\right)\left(\frac{1}{2}\frac{X}{G} - \frac{1}{6}\right) \approx 0 \tag{41}$$

and

$$\left.\begin{aligned} \frac{X_1}{G} &= \frac{1}{3} + \varepsilon_1 \\ \frac{X_2}{G} &= -\frac{M}{G} + \varepsilon_2 \end{aligned}\right\} \tag{42}$$

where

$$\varepsilon_1 = j\,\frac{\Omega^*}{9}\,\frac{(-5G^2 + 6 - 9\alpha_o)}{G(3G + 9M)} \tag{43}$$

$$\varepsilon_2 = -\left(\frac{\Omega^*}{9}\right)^2 A'B' - j\,\frac{\Omega^*}{9}\,A'$$

$$A' = \frac{M^3 + \frac{5}{6}GM^2 - M - \frac{3}{2}G^2M + G^3 - G(1 - \alpha_o)}{(-\frac{1}{2}GM - \frac{1}{6}G^2)} \tag{44}$$

$$B' = \frac{\begin{aligned}&[M^3 + \tfrac{5}{6}GM^2 - M + \tfrac{3}{2}G^2M + G^3 - G(1 - \alpha_o)]\ [-\tfrac{1}{2}G] \\ &-[-3M^2 - \tfrac{5}{6}GM + 1 - \tfrac{3}{2}G^2]\ [\tfrac{1}{2}GM + \tfrac{1}{6}G^2]\end{aligned}}{[-\frac{1}{2}GM - \frac{1}{6}G^2]^2}$$

Table 6 presents the kinematic wave characteristics for the flow regime, $\Omega^* << 1$ and $\Omega^* << G$.

From Tables 5 and 6, it can be seen that in the low frequency regime, the second kinematic wave characteristics are very complicated functions of M and G. The significance of this wave differs in different regimes of liquid velocity and relative velocity and it can be better observed from the numerical data as shown later in Figures 9 and 10.

Wave #1 (kinematic wave)

$$\frac{C_1 - V_{Lo}}{V_{Lo}} = (1 - \alpha_o)\frac{G}{M}$$

$$\frac{\eta_{R1}}{\left(\frac{\nu_L}{V_{Lo}R_o^2}\right)} = \frac{-3(2 - 3\alpha_o)MG^2}{2(M + (1 - \alpha_o)G)}$$

Wave #2 (kinematic wave)

$$\frac{C_2 - V_{Lo}}{V_{Lo}} = -\frac{A + MB}{MB}$$

$$\frac{\eta_{R2}}{\left(\frac{\nu_L}{V_{Lo}R_o^2}\right)} = +\frac{9M}{A}$$

$$A = \frac{[M^2(M + G)(M + 2G) - (1 - \alpha_o)(M + G)^2 - 3\alpha_o M^2]}{[-M^3 - \frac{5}{6}GM^2 + M + G(1 - \alpha_o)]}$$

$$B = \frac{\left\{-4M^3 - 9M^2G - 4MG^2 - 2(1 - \alpha_o)(M + G) + 6\alpha_o M\right\} \times \left\{-M^3 - \frac{5}{6}GM^2 + M + G(1 - \alpha_o)\right\} - \left\{3M^2 + \frac{5}{3}MG - 1\right\} \times \left\{M^2(M + G)(M + 2G) - (1 - \alpha_o)(M + G)^2 - 3\alpha_o M^2\right\}}{\left\{-M^3 - \frac{5}{6}GM^2 + M + G(1 - \alpha_o)\right\}^2}$$

Table 5. Kinematic waves for small relative velocity and low frequency such that $G << \Omega^* << 1$ for the low Reynolds number flow regime.

Wave #1 (kinematic wave)

$$\frac{C_1 - V_{Lo}}{V_{Lo}} = \frac{G}{3M}$$

$$\frac{\eta_{R1}}{\left(\frac{\nu_L}{V_{Lo}R_o^2}\right)} = \frac{-3\Omega^{*2}(-5G^2 + 6 - 9\alpha_o)M}{(3M + G)^3}$$

Wave #2 (kinematic wave)

$$\frac{C_2 - V_{Lo}}{V_{Lo}} = -\frac{A' + MB'}{MB'}$$

$$\frac{\eta_{R2}}{\left(\frac{\nu_L}{V_{Lo}R_o^2}\right)} = +\frac{9M}{A'}$$

$$A' = \frac{M^3 + \frac{5}{6}GM^2 - M + \frac{3}{2}G^2M + G^3 - G(1 - \alpha_o)}{\left(-\frac{1}{2}GM - \frac{1}{6}G^2\right)}$$

$$B' = \frac{\left[M^3 + \frac{5}{6}GM^2 - M + \frac{3}{2}G^2M + G^3 - G(1 - \alpha_o)\right]\left[-\frac{1}{2}G\right] - \left[-3M^2 - \frac{5}{6}GM + 1 - \frac{3}{2}G^2\right]\left[\frac{1}{2}GM + \frac{1}{6}G^2\right]}{\left[-\frac{1}{2}GM - \frac{1}{6}G^2\right]^2}$$

Table 6. Kinematic waves with relative velocity and low frequency such that $\Omega^* << 1$ and $\Omega^* << G$ for the low Reynolds number flow regime.

3.3. Waves with Mean Relative Velocity at High Reynolds Number

The high relative motion Reynolds number flow regime is perhaps of greater interest because most engineering bubbly two-phase flows fall into this category. Note, however, the similarity between the equations (11) and (12). At high relative motion Reynolds number flow, the frequency parameter Ω^* is replaced by the parameter $\frac{\Omega_c}{C_D G}$ which contains the ratio of the frequency parameter Ω_c and relative velocity parameter G. Other than this there are only minor changes in a few numerical coefficients. Hence the asymptotic solutions are very similar to those for low relative motion Reynolds number except that the zero gravity, or zero relative velocity case does not exist for high relative motion Reynolds number flows.

Tables 7 and 10 present the results of the asymptotic analyses for the high relative motion Reynolds number case in different relative velocity and frequency regimes. Now comparing the results presented in Tables 3 to 6 with those in Tables 7 to 10 for wave characteristics in low and high relative motion Reynolds number flows respectively, it can be seen that for both Reynolds number regimes, the wave speeds are identical for the corresponding relative motion and frequency regime except in the corresponding cases when $\Omega^* \ll 1$ and $\Omega^* \ll G$ (for low relative motion Reynolds number) corresponding to $\Omega_c/C_D G \ll 1$ and $\Omega_c/C_D \ll G^2$ (for high relative motion Reynolds number). In both cases, the wave speeds contain the same functions of relative velocity G and liquid velocity M. However, some of the numerical coefficients in the functions are different due to the different order of dependence of drag force or relative velocity and bubble radius (see equation (5)).

The main difference in the wave characteristics between low and high relative motion Reynolds number is exhibited in the wave attenuation, η_R. Since the drag force at high relative Reynolds number is proportional to the square of relative velocity and bubble radius while low relative motion Reynolds number drag is linearly proportional to relative velocity and bubble velocity, the wave attenuation in the high relative motion Reynolds number regime is subjected to one order higher dependence on G and R than that of the low relative motion Reynolds number regime.

In all of the above data, the wave information for the case $G \ll 1$ and $\Omega_c/C_D G \gg 1$ (as presented in Table 7) presents the case which usually occurs. This is due to the fact that G is usually of the order of 10^{-3} and $\Omega_c = \Omega R_o/C_o$ is of the order of 10^{-4} to 10^{-1} when frequency regime of most engineering concern is of the order of 0.1 to 100 Hz; the bubble radius is of the order of $\frac{1}{8}$ in. and the liquid velocity is of the order of 1 ft/sec. Then the parameter $\Omega_c/C_D G$ is of the order of 10^{-1} to 10^{2}.

Wave #1 (kinematic wave)

$$\frac{C_1 - V_{Lo}}{V_{Lo}} = \frac{G}{M}(1 - \alpha_o)\left[\frac{G + M}{G(1 - \alpha_o) + M(1 + 2\alpha_o)}\right]$$

$$\frac{\eta_{R1}}{\left(\frac{C_o}{V_{Lo}R_o}\right)} = \frac{\Omega_c MG\sqrt{3\alpha_o(1 - \alpha_o)}}{M^2(1 + 2\alpha_o) + 2MG(1 - \alpha_o) + G^2(1 - \alpha_o)}$$

Wave #2 (kinematic wave)

$$\frac{C_2 - V_{Lo}}{V_{Lo}} = \frac{G}{M}(1 - \alpha_o)\left[\frac{G + M}{G(1 - \alpha_o) + M(1 + 2\alpha_o)}\right]$$

$$\frac{R2}{\left(\frac{C_o}{V_{Lo}R_o}\right)} = \frac{-\Omega_c MG\sqrt{3\alpha_o(1 - \alpha_o)}}{M^2(1 + 2\alpha_o) + 2MG(1 - \alpha_o) + G^2(1 - \alpha_o)}$$

Wave #3 (dynamic wave)

$$\frac{C_3 - V_{Lo}}{C_o} = \sqrt{1 + 2\alpha_o} + \frac{1 + 8\alpha_o}{2(1 + 2\alpha_o)}G$$

$$\frac{\eta_{R3}}{\left(\frac{1}{R_o}\right)} = -\frac{3C_DG}{2}\frac{\left[\alpha_o - \frac{(1 + 38\alpha_o)G}{24\sqrt{1 + 2\alpha_o}}\right]}{(1 + 2\alpha_o)(\sqrt{1 + 2\alpha_o} + M)}$$

Wave #4 (dynamic wave)

$$\frac{C_3 - V_{Lo}}{C_o} = -\sqrt{1 + 2\alpha_o} + \frac{1 + 8\alpha_o}{2(1 + 2\alpha_o)}G$$

$$\frac{\eta_{R4}}{\left(\frac{1}{R_o}\right)} = +\frac{3C_DG}{2}\frac{\left[\alpha_o - \frac{(1 + 38\alpha_o)G}{24\sqrt{1 + 2\alpha_o}}\right]}{(1 + 2\alpha_o)(\sqrt{1 + 2\alpha_o} - M)}$$

Table 7. Waves for small relative velocity ($G \ll 1$) and high frequency ($\Omega_c/C_DG \gg 1$) for the high Reynolds number flow regime.

Wave #1 (kinematic wave)

$$\frac{C_1 - V_{Lo}}{V_{Lo}} = \frac{G}{M}$$

$$\frac{\eta_{R1}}{\left(\frac{C_o}{V_{Lo}R_o}\right)} = \frac{C_D G}{4} \frac{M}{M + G}$$

Wave #2 (kinematic wave)

$$\frac{C_2 - V_{Lo}}{V_{Lo}} = \frac{2G}{M}$$

$$\frac{\eta_{R2}}{\left(\frac{C_o}{V_{Lo}R_o}\right)} = - \frac{C_D G}{4} \frac{7M}{(M + 2G)}$$

Wave #3 (dynamic wave)

$$\frac{C_3 - V_{Lo}}{C_o} = \sqrt{\frac{1 - \alpha_o}{2}}$$

$$\frac{\eta_{R3}}{\left(\frac{1}{R_o}\right)} = \left(\frac{3C_D}{4}\right) \frac{G^2}{\sqrt{2(1 - \alpha_o)}\left(\sqrt{2(1 - \alpha_o)} - 2M\right)}$$

Wave #4 (dynamic wave)

$$\frac{C_4 - V_{Lo}}{C_o} = \sqrt{\frac{1 - \alpha_o}{2}}$$

$$\frac{\eta_{R4}}{\left(\frac{1}{R_o}\right)} = + \left(\frac{3C_D}{4}\right) \frac{G^2}{\sqrt{2(1 - \alpha_o)}\left(\sqrt{2(1 - \alpha_o)} - 2M\right)}$$

Table 8. Waves for high relative velocity ($G \gg 1$) and high frequency ($\Omega_c/C_D G \gg 1$) for the high Reynolds number flow regime.

Wave #1 (kinematic wave)

$$\frac{C_1 - V_{Lo}}{V_{Lo}} = \frac{G}{M}(1 - \alpha_o)$$

$$\frac{\eta_{R1}}{\left(\frac{C_o}{V_{Lo}R_o}\right)} = \frac{-C_D}{16}\,\frac{(1 - 6\alpha_o)G^3M}{(M + (1 - \alpha_o)G)}$$

Wave #2 (kinematic wave)

$$\frac{C_2 - V_{Lo}}{V_{Lo}} = -\frac{A + MB}{MB}$$

$$\frac{\eta_{RI}}{\left(\frac{C_o}{V_{Lo}R_o}\right)} = \frac{3C_DG}{2}\,\frac{M}{A}$$

$$A = \frac{M^2(M + G)(M + 2G) - (1 - \alpha_o)(M + G)^2 - 3\alpha_oM^2}{-M^3 - \frac{13}{12}GM^2 + M + G(1 - \alpha_o)}$$

$$B = \frac{\begin{array}{c}-[M^2(M + G)(M + 2G) + (1 - \alpha_o)(M + G)^2 - 3\alpha_oM^2] \times \\ [3M^2 + \frac{13}{6}MG - 1] + [-4M^3 - 9M^2G - 4MG^2 - \\ 2(1 - \alpha_o)(M + G) + 6\alpha_oM] \times [-M^3 - \frac{13}{12}GM^2 + M + G(1 - \alpha_o)]\end{array}}{[-M^3 - \frac{13}{12}GM^2 + M + G(1 - \alpha_o)]^2}$$

Table 9. Kinematic waves for small relative velocity and low frequency such that $(G << \Omega_c/C_DG << 1)$ for the high Reynolds number flow regime.

Wave #1 (kinematic wave)

$$\frac{C_1 - V_{Lo}}{V_{Lo}} = \frac{5}{6}\frac{G}{M}$$

$$\frac{\eta_{R1}}{\left(\frac{C_o}{V_{Lo}R_o}\right)} = \frac{-\Omega_c^{\,2}}{C_D}\,\frac{(-7G^2 + 24 - 144\alpha_o)M}{(6M + 5G)^3\,G}$$

Wave #2 (kinematic wave)

$$\frac{C_2 - V_{Lo}}{V_{Lo}} = -\frac{A' + MB'}{MB}$$

$$\frac{\eta_{R2}}{\left(\frac{C_o}{V_{Lo}R_o}\right)} = \frac{3C_DG}{2}\,\frac{M}{A'}$$

$$A' = \frac{M^3 + \frac{13}{12}GM^2 - M + \frac{3}{4}G^2M + \frac{1}{2}G^3 - G(1 - \alpha_o)}{-\frac{1}{4}GM - \frac{5}{24}G^2}$$

$$B' = \frac{\begin{array}{c}-\left[M^3 + \frac{13}{12}GM^2 - M + \frac{3}{4}G^2M + \frac{1}{2}G^2 - G(1 - \alpha_o)\right]\left[\frac{1}{4}G\right] \\ + \left[3M^2 + \frac{13}{6}MG - 1 + \frac{3}{4}G^2\right]\left[\frac{1}{4}GM + \frac{5}{24}G^2\right]\end{array}}{\left[-\frac{1}{4}GM - \frac{5}{24}G^2\right]^2}$$

Table 10. Kinematic waves for relative velocity and low frequency such that $\Omega_c/C_DG \ll 1$ and $\Omega_c/C_D \ll G^2$ for the high Reynolds number flow regime.

IV. PRESENTATION OF NUMERICAL DATA

In this section, numerical data of wave characteristics are presented in graphical form. The purpose of this is to illustrate the nature of the transitional results in between the asymptotic regimes described in detail in the preceding sections.

4.1. Wave Characteristics for Zero Mean Relative Velocity

Wave characteristics for the zero gravity, zero mean relative velocity flow regime are plotted against reduced frequency Ω^* in Figures 1 to 6. Results for a few selected values of Mach numbers (M) and void fractions (α_o) are shown. It can be seen that the numerical results at their asymptotic frequency regimes match well with the analytic solutions as presented in Tables 1 and 2. The transitional results lie in the reduced frequency domain $\Omega^* = 0.6 \rightarrow 20$ for kinematic waves and $1 \rightarrow 100$ for dynamic waves approximately.

4.2. Wave Characteristics for Mean Relative Velocity at Low Reynolds Number

Wave characteristics for low relative motion Reynolds number flow regime are plotted against reduced frequency Ω^* in Figures 7 to 14. For kinematic waves, the nondimensional wave speed $\frac{C - V_{Lo}}{V_{Lo}}$ and attenuation $n_R/(\nu_L/\nu_{Lo}R_o)$ for some typical relative velocity to liquid velocity ratios (G*) are shown. However, for dynamic waves, the nondimensional wave speed $\frac{C - V_{Lo}}{C_o}$ and the attenuation $n_R/(\nu_L/C_oR_o)$ for liquid Mach number $M = 0$ and selected G values are shown instead.

The change of parameter used in characterizing different waves is due to the fact that kinematic wave characteristics are well defined functions of G^* while the dynamic wave characteristics are functions of both G and M. (See Tables 3 to 6).

From Figures 7 to 14, it can be seen that the transition frequencies between asymptotic solutions change considerably with the values of G^* or G selected. In order to provide better understanding of wave characteristics in different frequency regimes, each wave system is now considered in more detail.

For kinematic waves, the transition frequency domain lies within $\Omega^* = 10^{-3} \rightarrow 1$ when G^* is small; however as G^* becomes larger, the transition frequency changes considerably. The first kinematic wave travels downstream at all frequencies (see Figure 7) yet the wave is amplified at high frequency and attenuated at low frequency (see Figure 8). Selecting the case $G^* = 1$ and $\alpha_o = 0.1$ as an example, the data of Figure 8 show that when reduced frequency Ω^* is larger than 2, the first kinematic wave is amplified as it travels downstream and for Ω^* smaller than 2, the wave is attenuated. The second kinematic wave has different directions of travel in different frequency regimes with the sign of its attenuation unchanged (see Figures 9 and 10). For small G^*, when Ω^* is larger than 10^{-1}, the second kinematic wave is attenuated as it travels downstream. But, when Ω^* is smaller than 10^{-1}, the wave travels upstream and is amplified as it proceeds.

For dynamic waves, since the wave speed in the low frequency regime is obtained from second order perturbation values, numerically computed data for dynamic wave speeds in this frequency regime are not dependable

and therefore, not presented in Figures 11 and 13. However, it still can be observed that the high frequency asymptotic results for dynamic waves (as presented in Tables 3 and 4) become valid at reduced frequencies Ω^* larger than G. Restricting the discussion to the high frequency regime, both dynamic waves are attenuated in their directions of travel.

It should be noted that in Figures 7 to 14, the wave characteristics are plotted against reduced frequency with a selected void fraction $\alpha_o = 0.1$ only. From the tables of the previous section which illustrate the asymptotic wave characteristics, it can be seen that the magnitude of the void fraction has an important effect on the wave characteristics. For example (see Tables 5 and 6)

$$\frac{C_1 - V_{Lo}}{V_{Lo}} = \begin{cases} (1 - \alpha_o)\frac{G}{M} & \text{at} \quad G << \Omega^* << 1 \\ \frac{G}{3M} & \text{at} \quad \Omega^* << 1 \text{ and } \Omega^* << G \end{cases}$$

$$\frac{\eta_{R1}}{(\frac{\nu_L}{V_{Lo}R^2})} = \begin{cases} \frac{-3(2 - 3\alpha_o)MG^2}{2(M + (1 - \alpha_o)G)} & \text{at} \quad G << \Omega^* << 1 \\ \frac{-3\Omega^{*2}(-5G^2 + 6 - 9\alpha_o)M}{(3M + G)^3} & \text{at} \quad \Omega^* << 1 \text{ and } \Omega^* << G \end{cases}$$

It can be observed that when the void fraction is larger than a certain value, the amplitude of the kinematic wave will grow as the wave travels downstream. Hence a kinematic shock will tend to develop in these low frequency regimes.

4.3. Wave Characteristics for Mean Relative Velocity at High Reynolds Number

Wave characteristics for high relative motion Reynolds number flow regime are plotted against reduced frequency $\frac{\Omega_c}{C_D G}$ in Figures 15 to 22. Similarity between asymptotic wave characteristics (see Tables 3 to 10) and numerical data (see Figures 7 to 22) can be observed for high and low relative motion Reynolds number flow regimes. Therefore, a similar discussion as given in section 4.3 can be applied here. However, it should be noted that due to the high order dependence on relative velocity, and hence G, for high relative motion Reynolds number drag, the wave characteristic parameters become different. That is $\frac{\eta_R}{\frac{C_o}{V_{Lo} R_o}}$ for kinematic wave attenuation and $\eta_R/[(V_{Go} - V_{Lo})/C_o R_o]$ for dynamic wave attenuation.

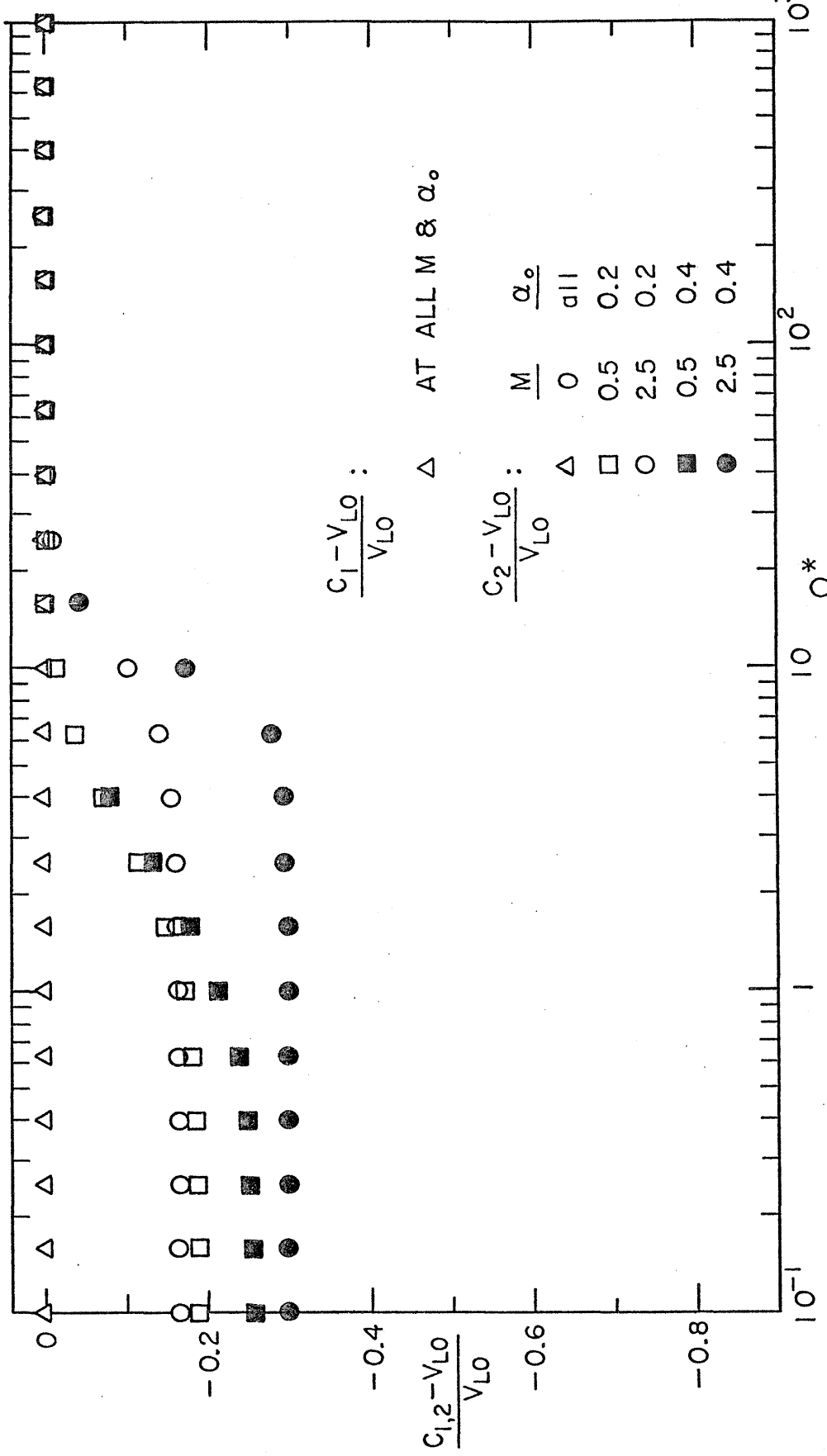

Figure 1. Non-dimensional kinematic wave speeds as functions of reduced frequency Ω^* in the zero gravity, zero relative velocity flow regime.

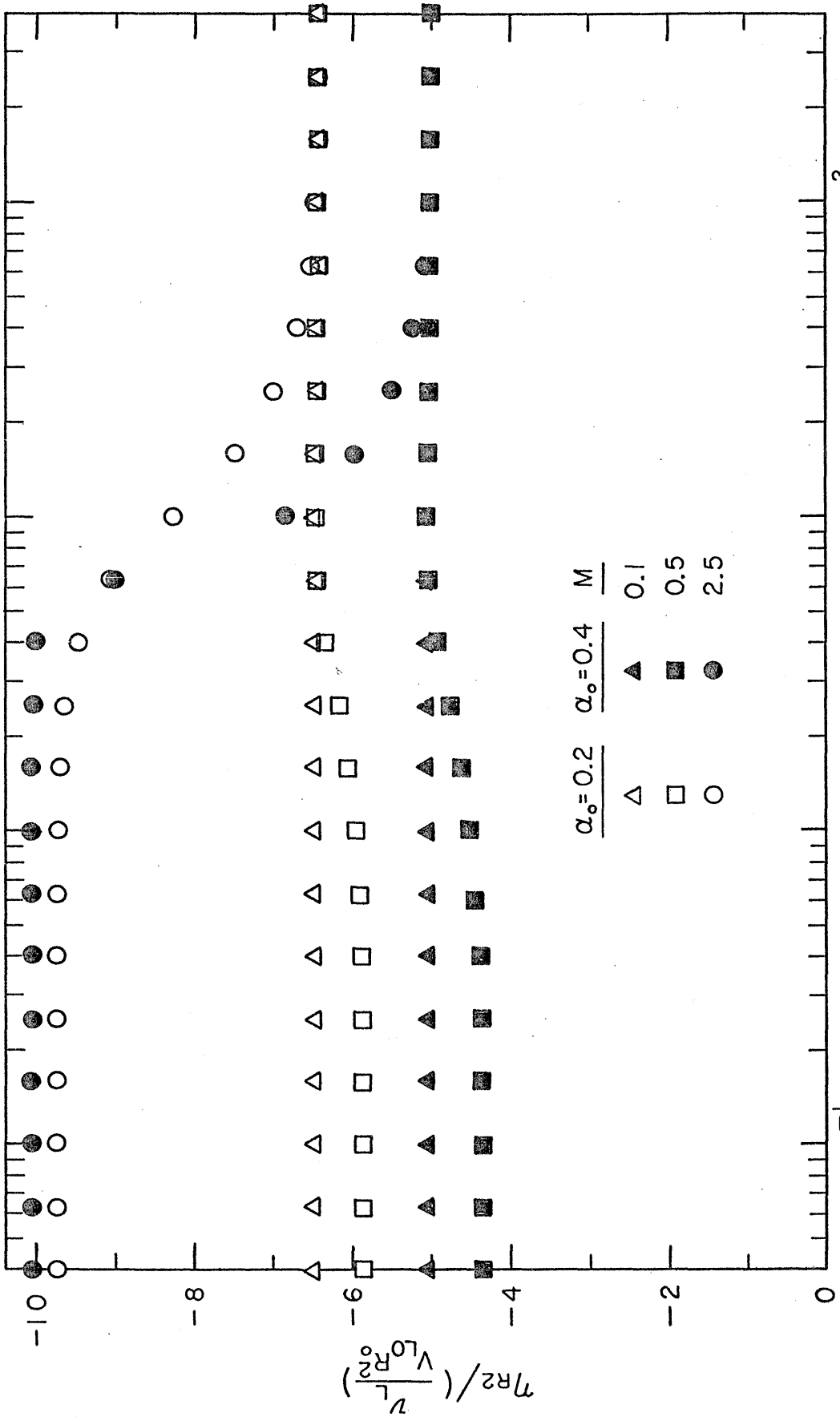

Figure 2. Non-dimensional attenuation of the second kinematic wave as a function of reduced frequency Ω^* in the zero gravity, zero relative velocity flow regime.

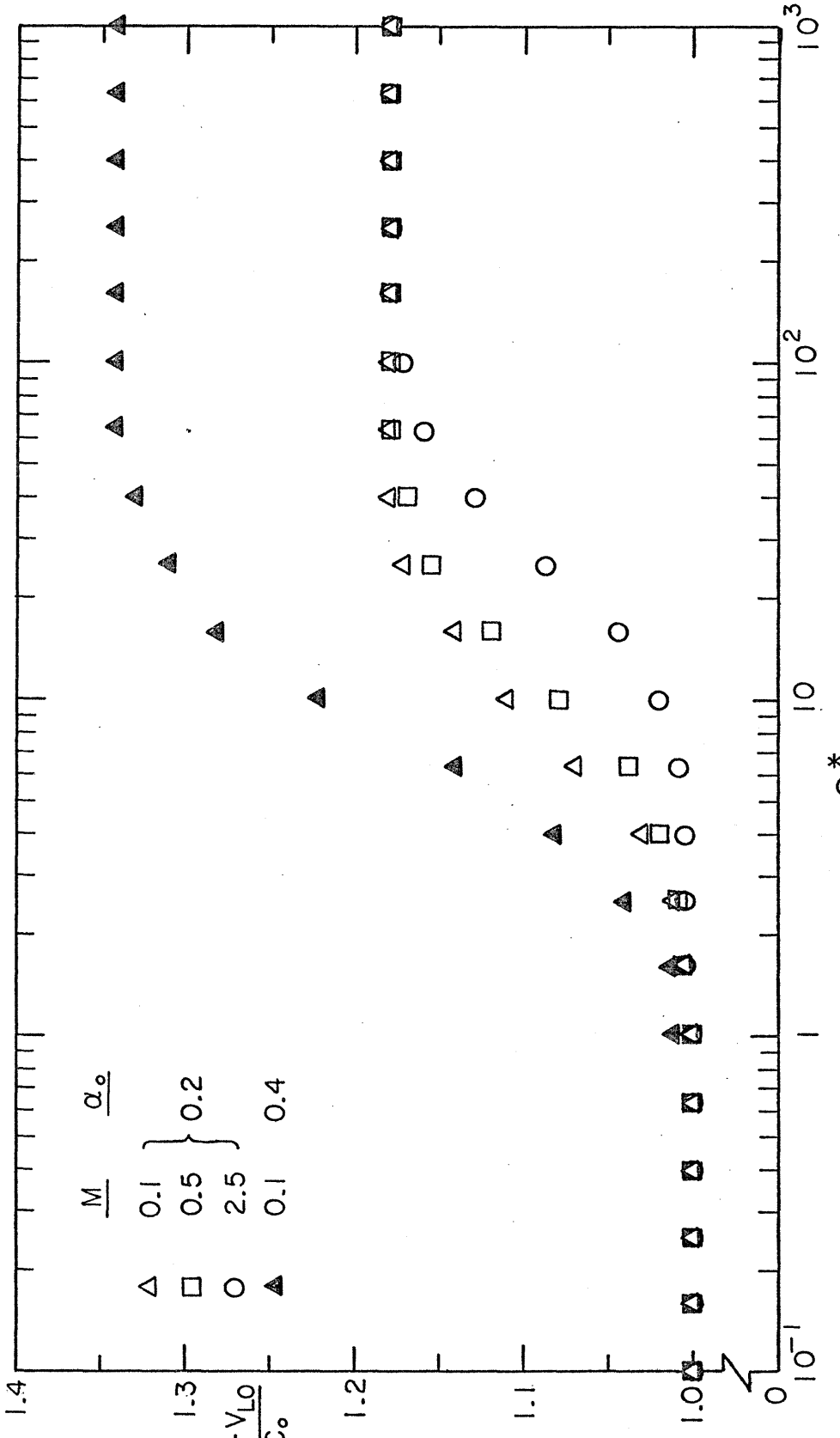

Figure 3. Non-dimensional downstream dynamic wave speed as a function of reduced frequency Ω^* in the zero gravity and zero relative velocity flow regime.

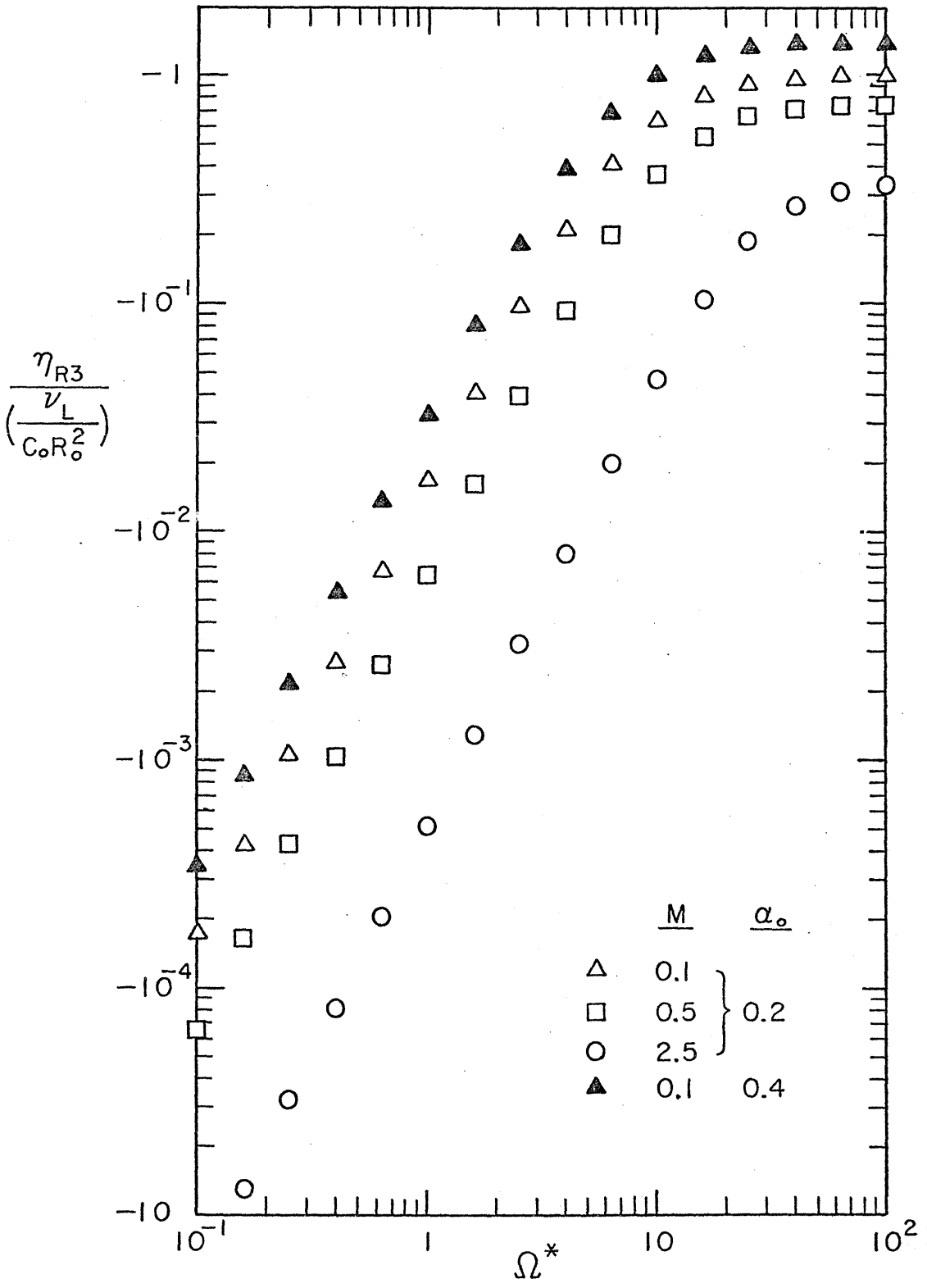

Figure 4. Non-dimensional attenuation of downstream dynamic wave as a function of reduced frequency Ω^* in the zero gravity, zero relative velocity flow regime.

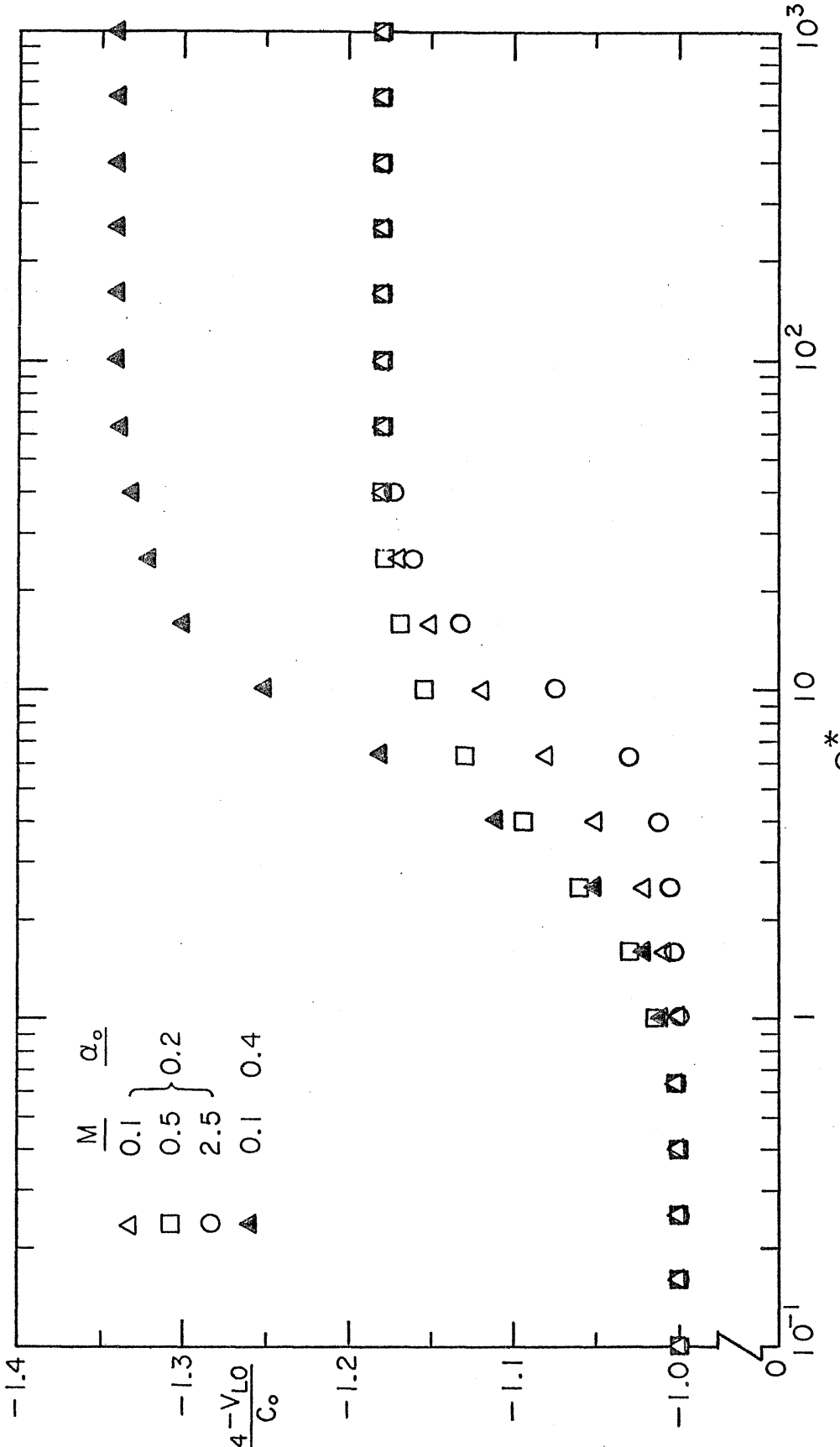

Figure 5. Non-dimensional upstream dynamic wave speed as a function of reduced frequency Ω^* in the zero gravity, zero relative velocity flow regime.

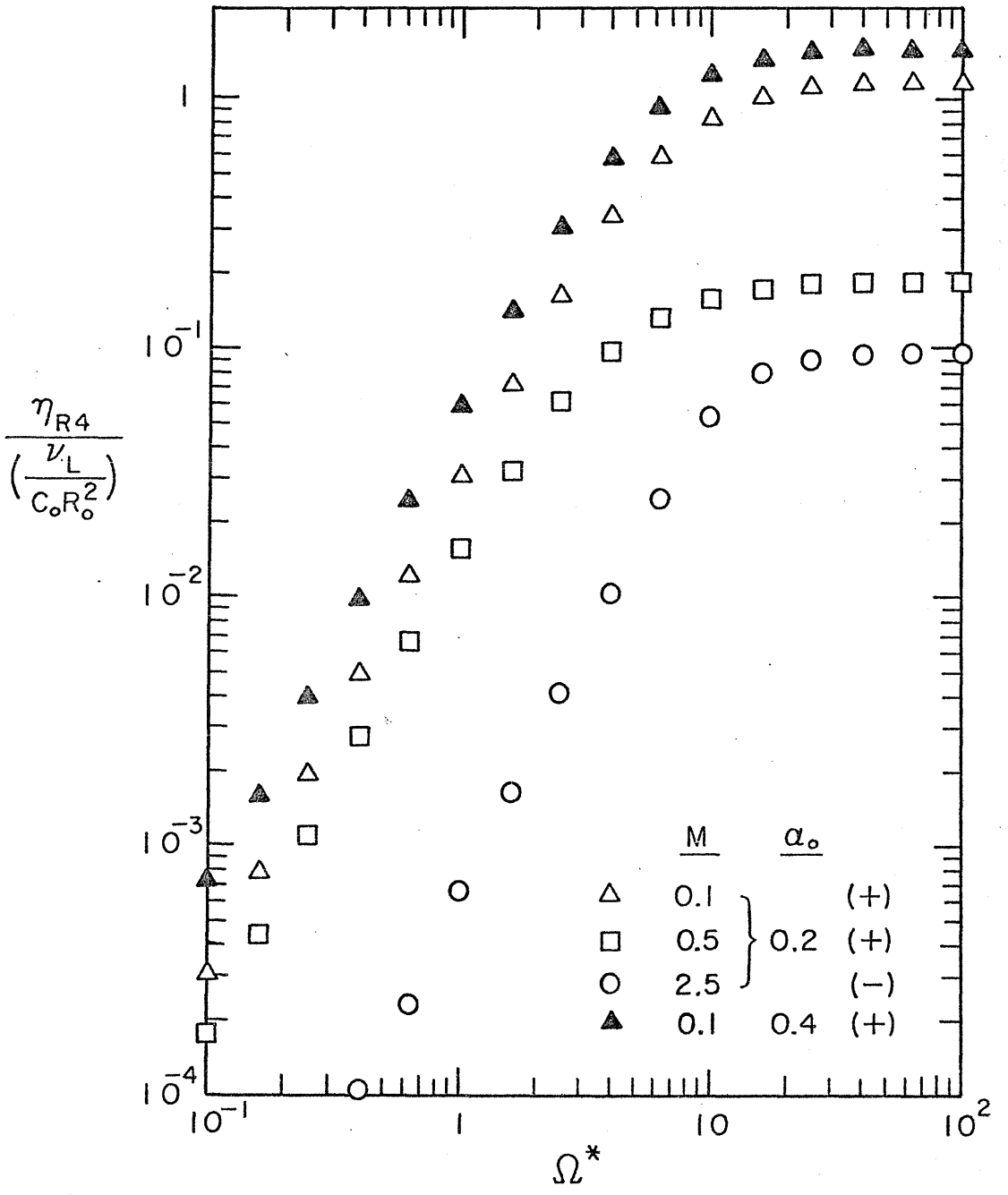

Figure 6. Non-dimensional attenuation of upstream dynamic wave as a function of reduced frequency Ω^* at zero gravity, zero relative velocity flow regime.

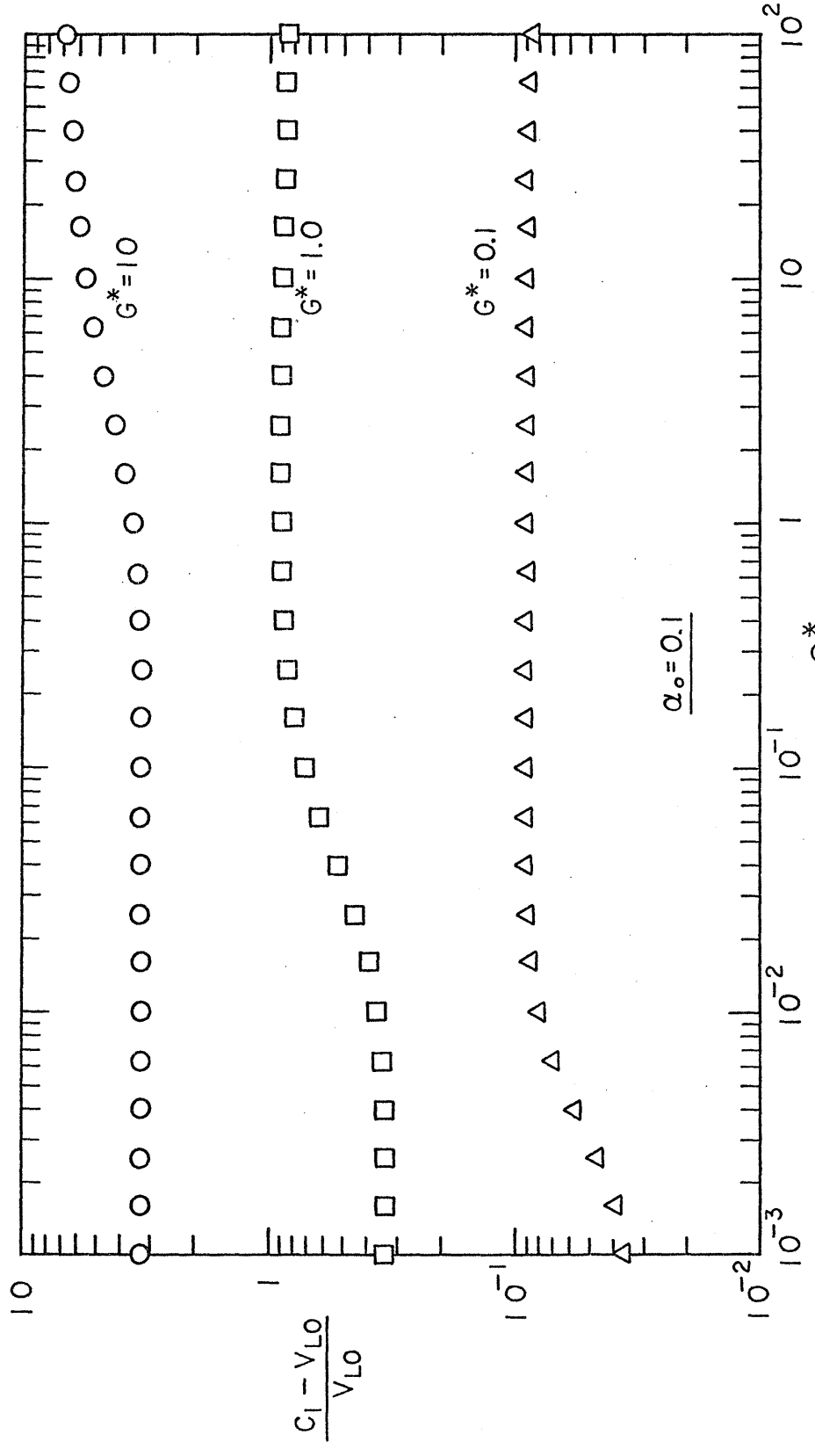

Figure 7. Non-dimensional first kinematic wave speed as a function of reduced frequency Ω^* in the low relative motion Reynolds number flow regime.

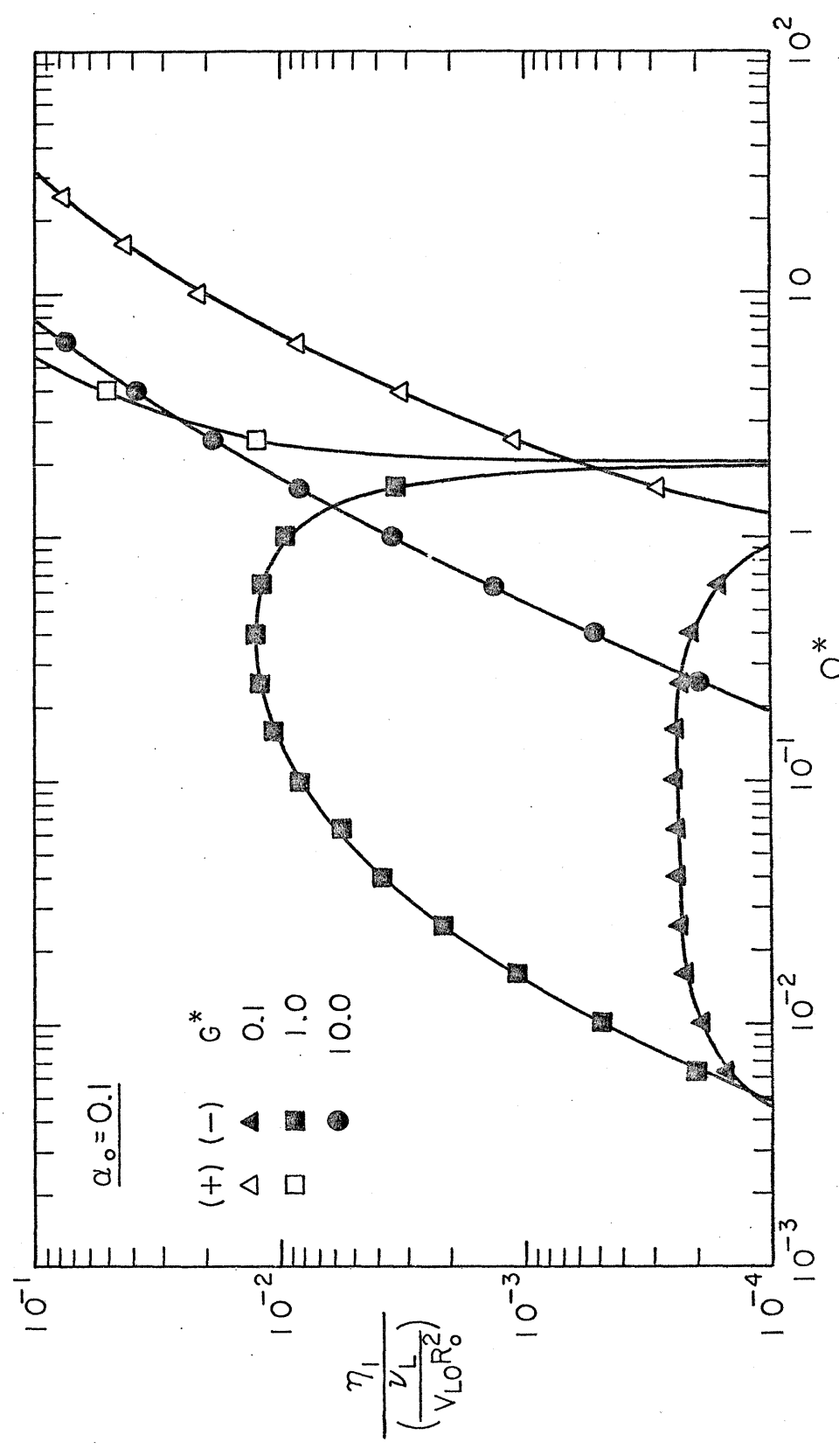

Figure 8. Non-dimensional attenuation of first kinematic wave as a function of reduced frequency Ω^* in the low relative motion Reynolds number flow regime.

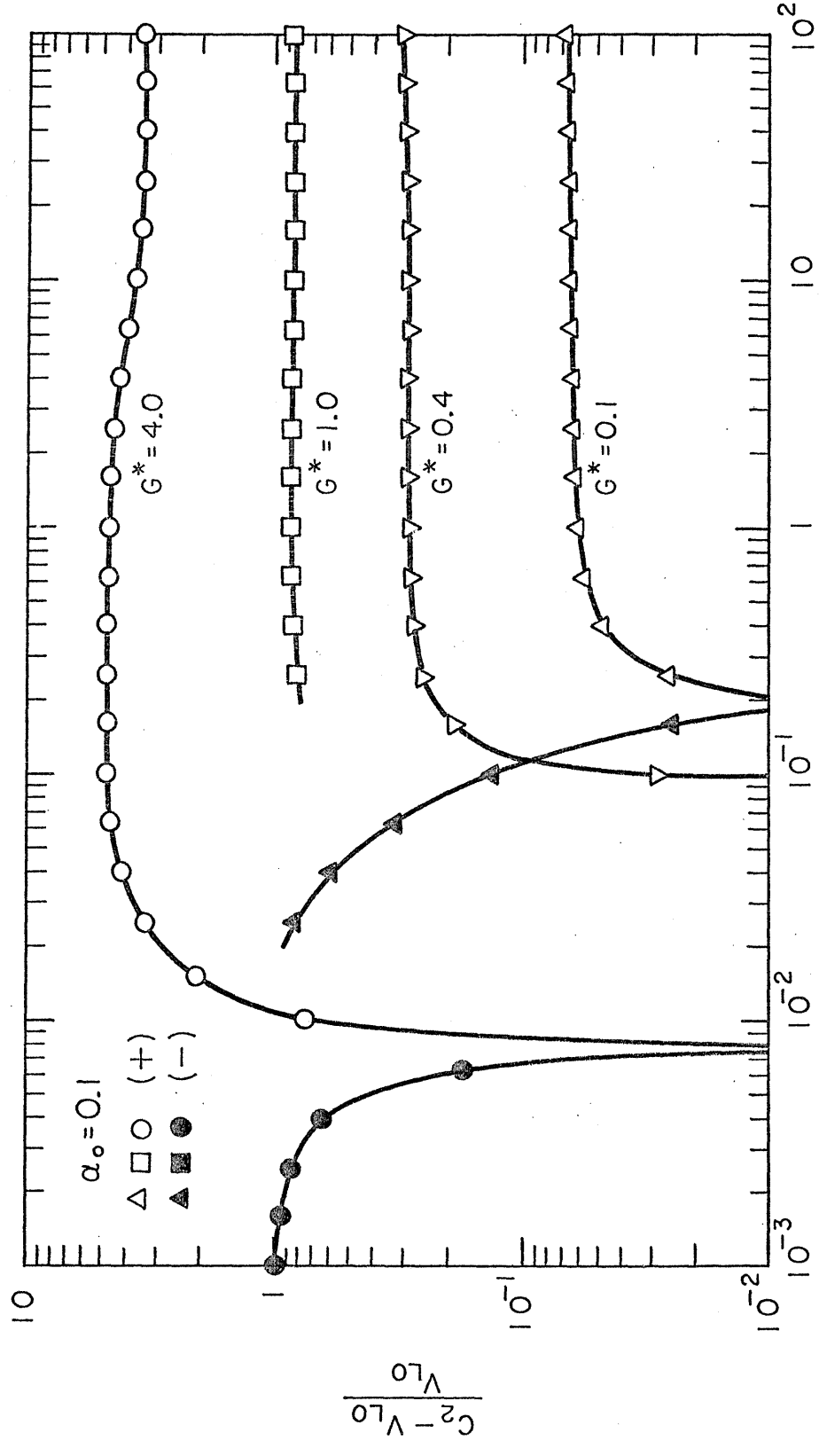

Figure 9. Non-dimensional second kinematic wave speed as a function of reduced frequency Ω^* in the low relative motion Reynolds number flow regime.

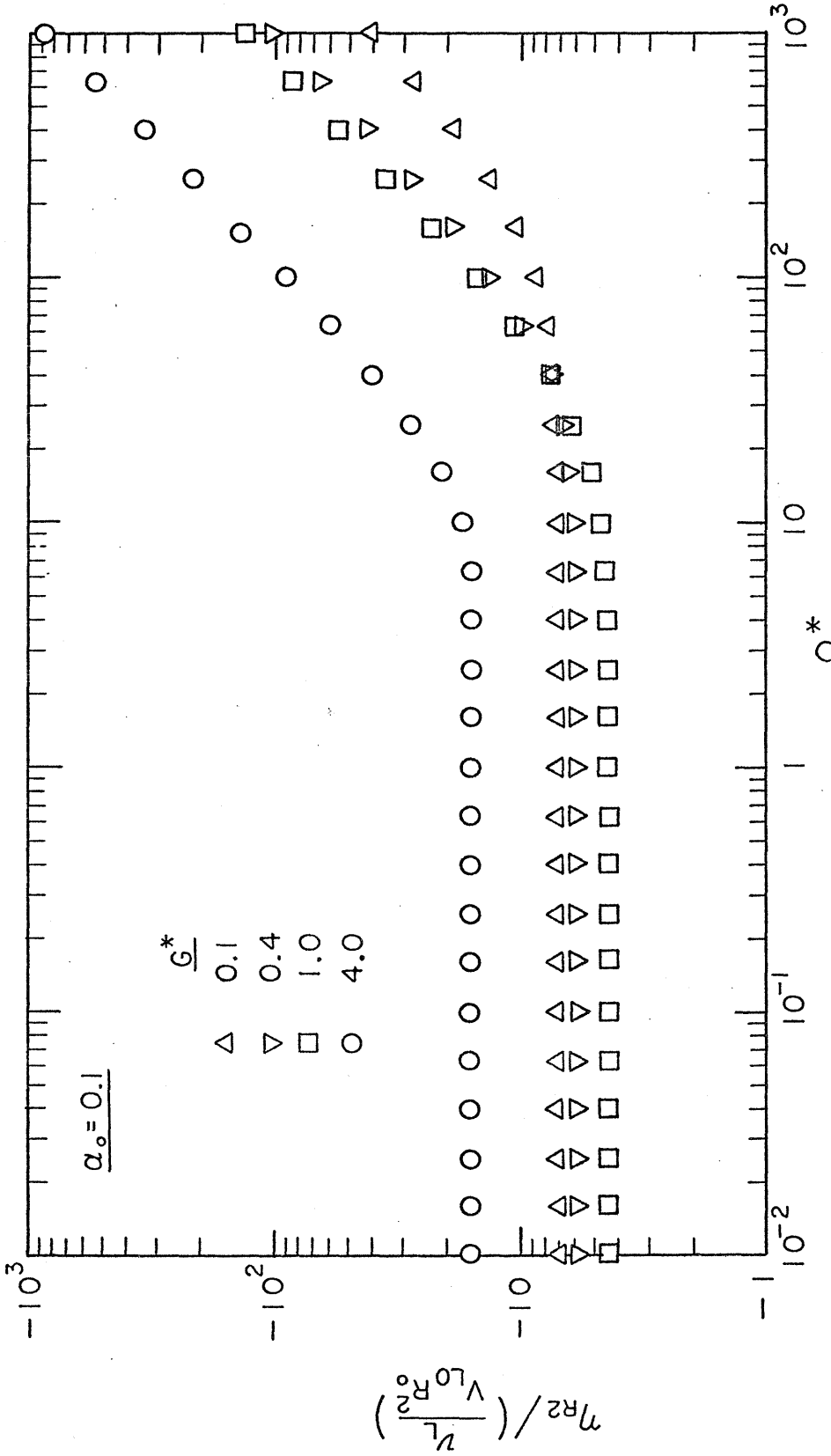

Figure 10. Non-dimensional attenuation of second kinematic wave as a function of reduced frequency Ω^* in the low relative motion Reynolds number flow regime.

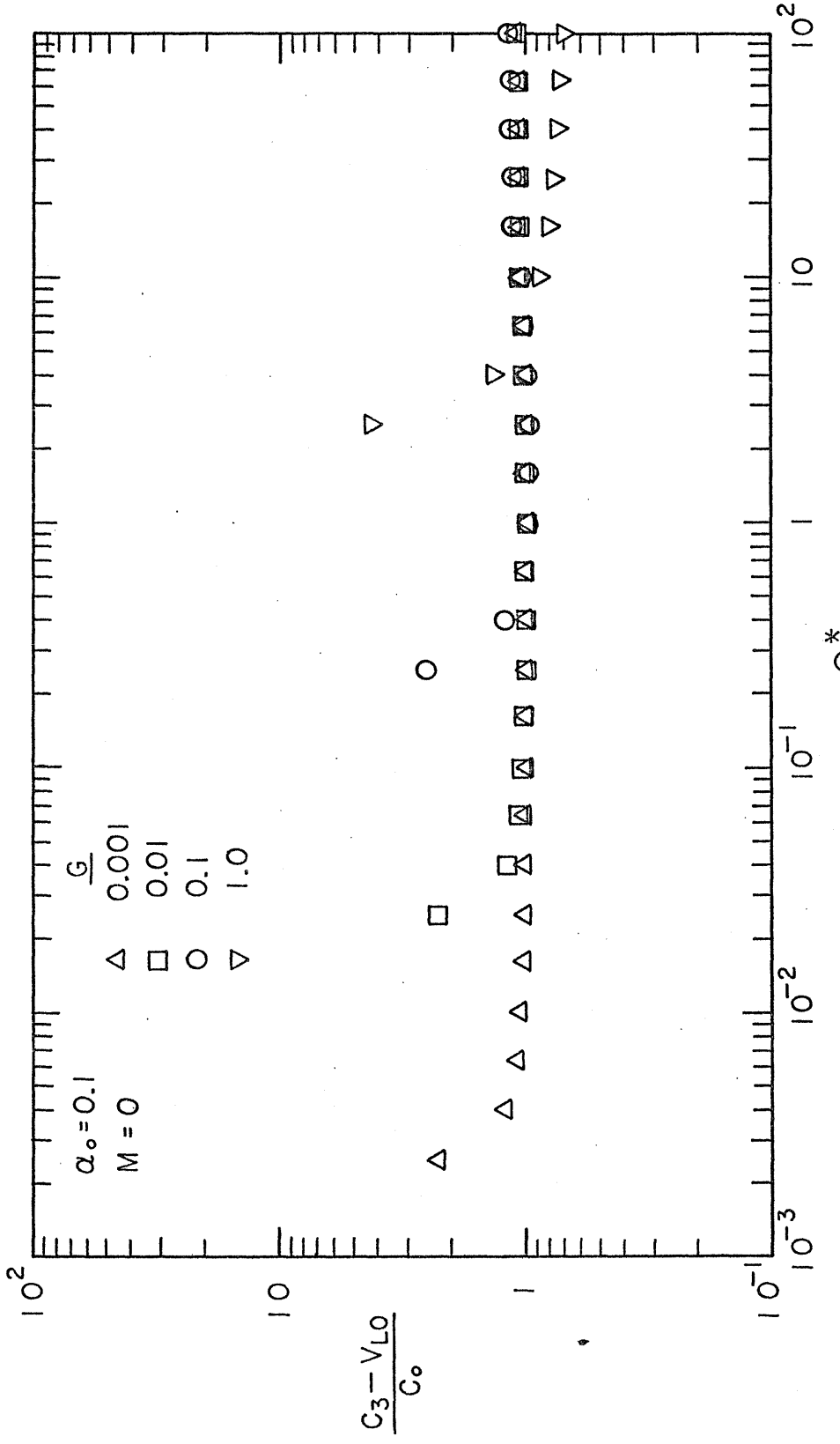

Figure 11. Non-dimensional downstream dynamic wave speed as a function of reduced frequency Ω^* in the low relative motion Reynolds number flow regime.

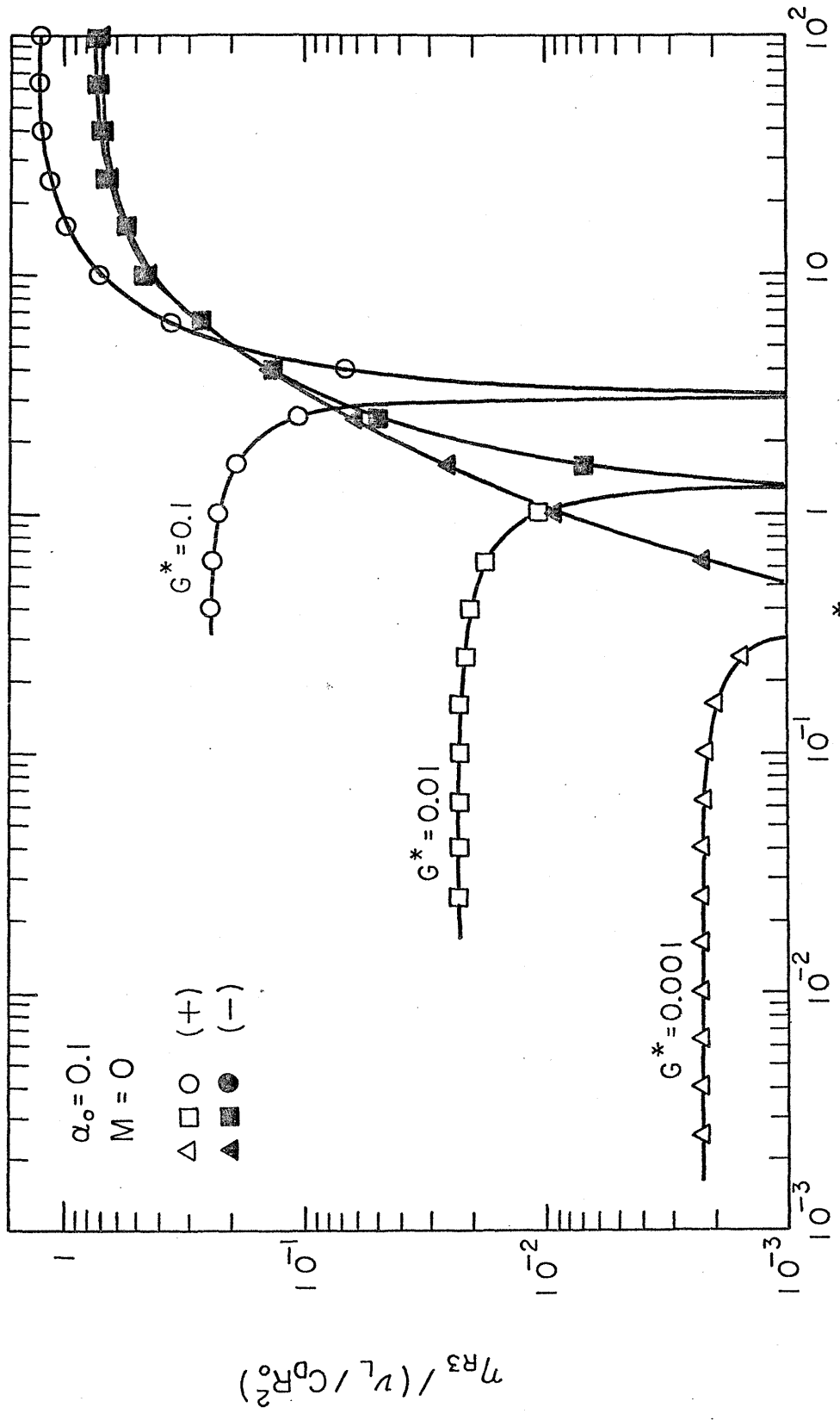

Figure 12. Non-dimensional attenuation of downstream dynamic wave as a function of reduced frequency Ω^* in the low relative motion Reynolds number flow regime.

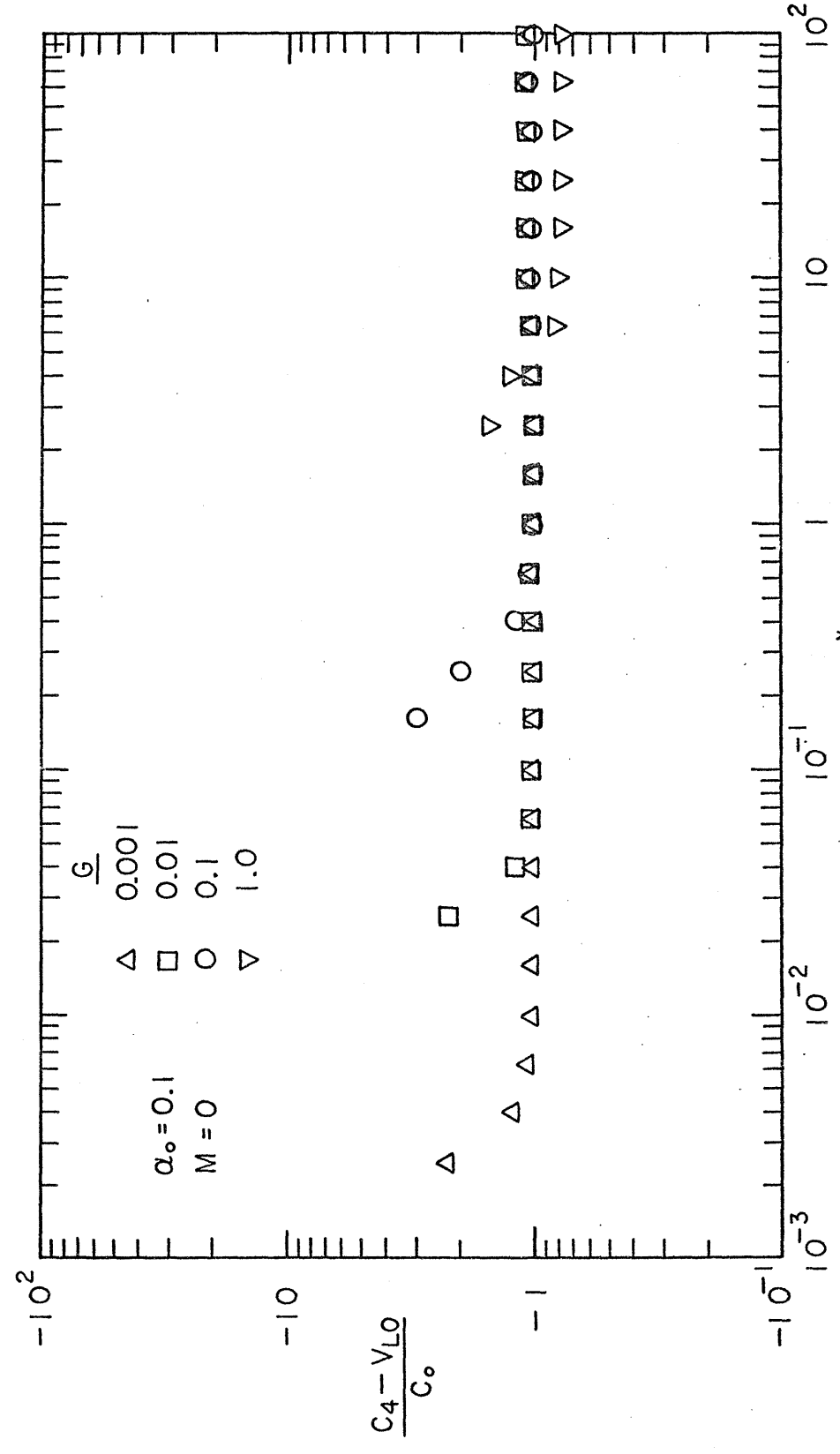

Figure 13. Non-dimensional upstream dynamic wave speed as a function of reduced frequency Ω^* in the low relative motion Reynolds number flow regime.

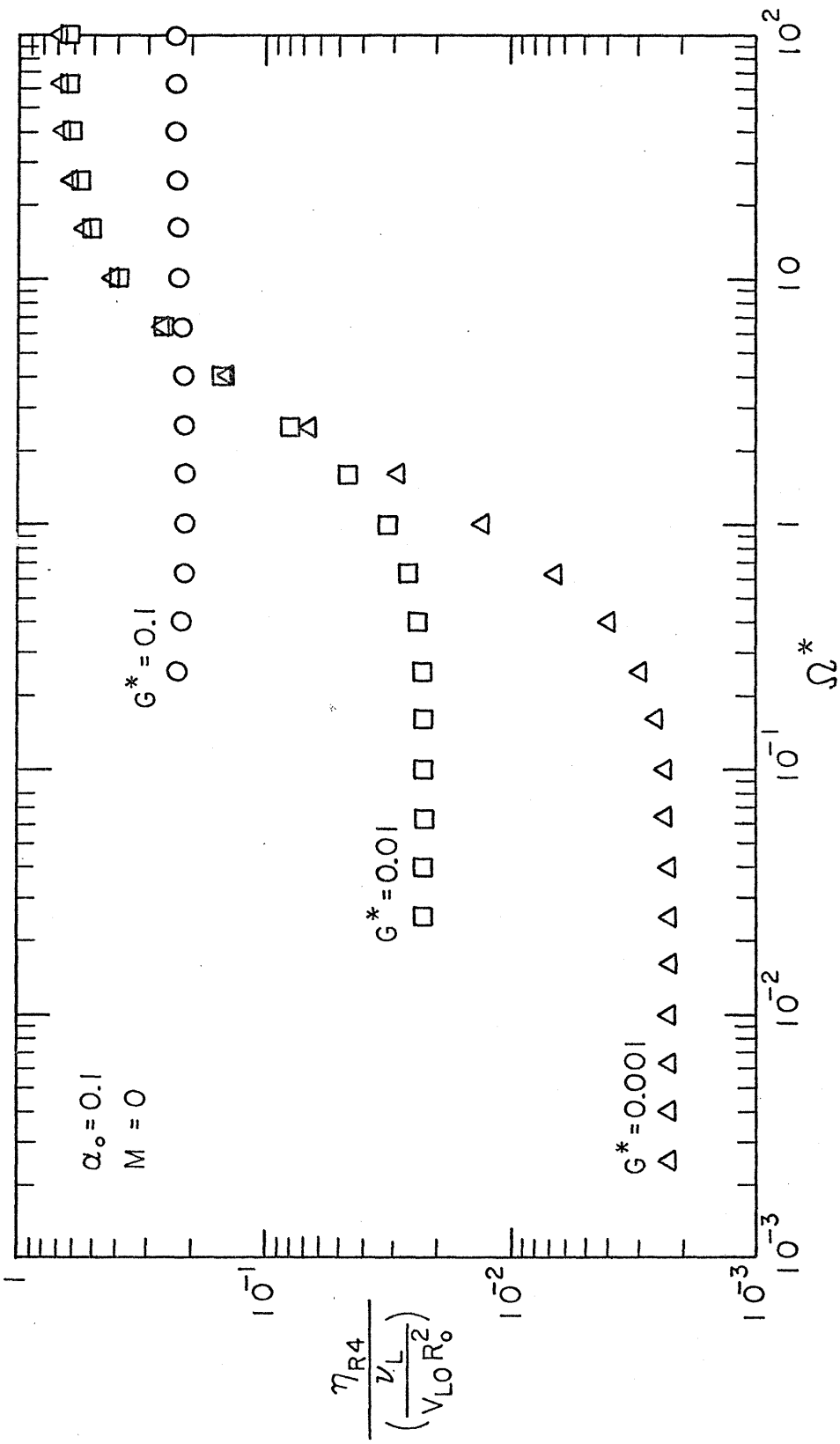

Figure 14. Non-dimensional attenuation of upstream dynamic wave as a function of reduced frequency Ω^* in the low relative motion Reynolds number flow regime.

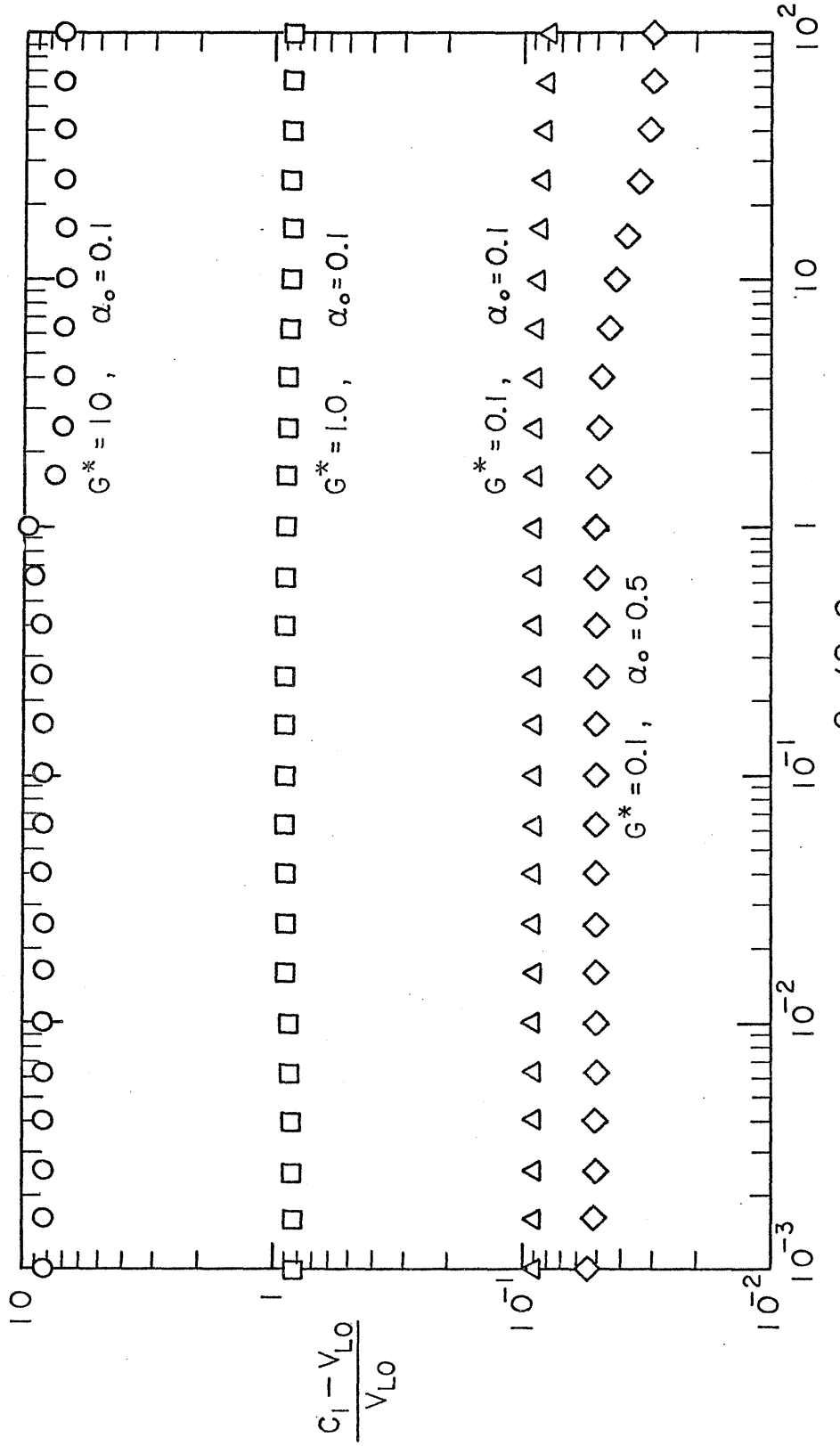

Figure 15. Non-dimensional first kinematic wave speed as a function of reduced frequency Ω_c/C_DG in the high relative motion Reynolds number flow regime.

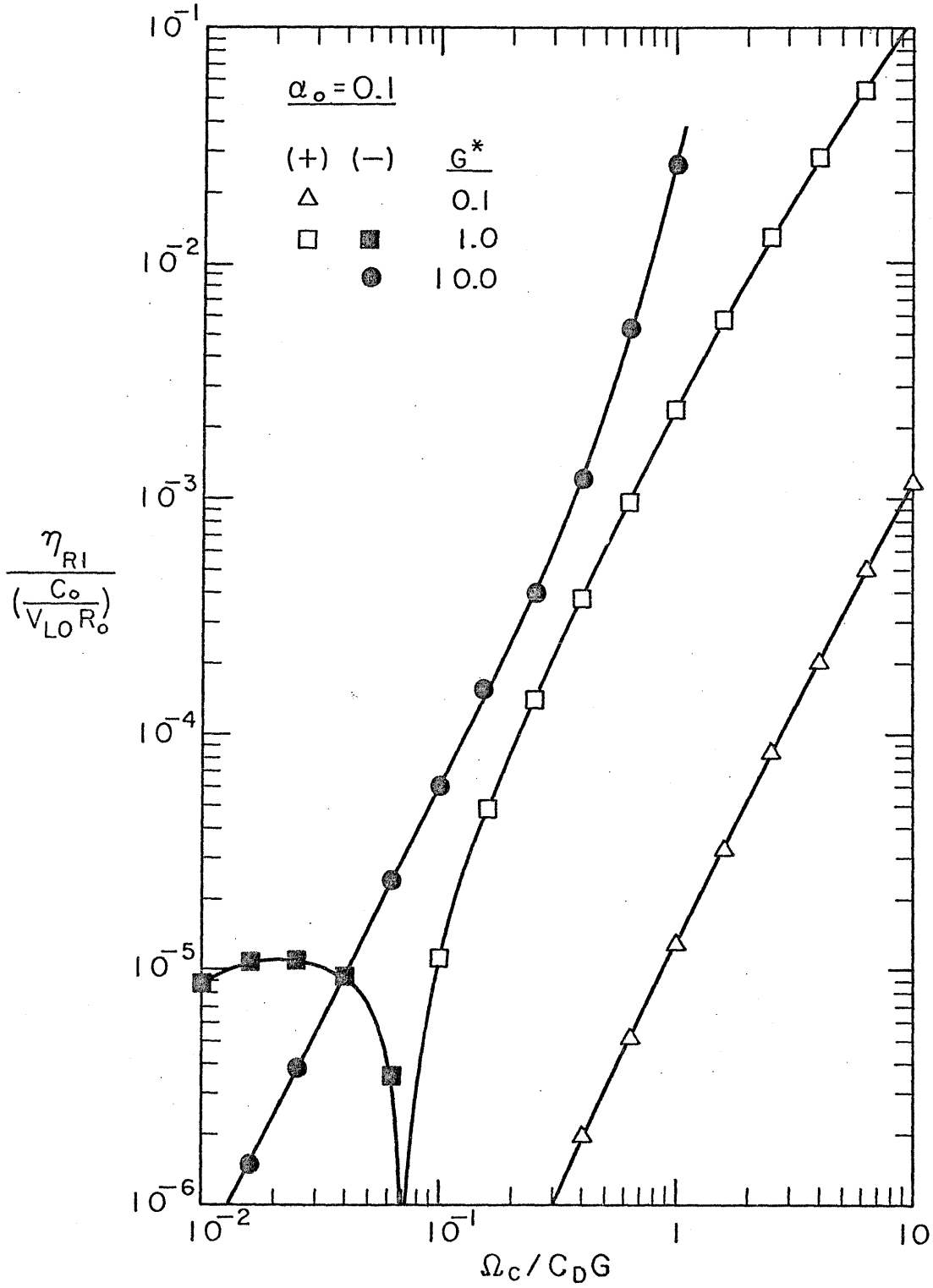

Figure 16. Non-dimensional attenuation of first kinematic wave as a function of reduced frequency $\Omega_C/C_D G$ in the high relative motion Reynolds number flow regime.

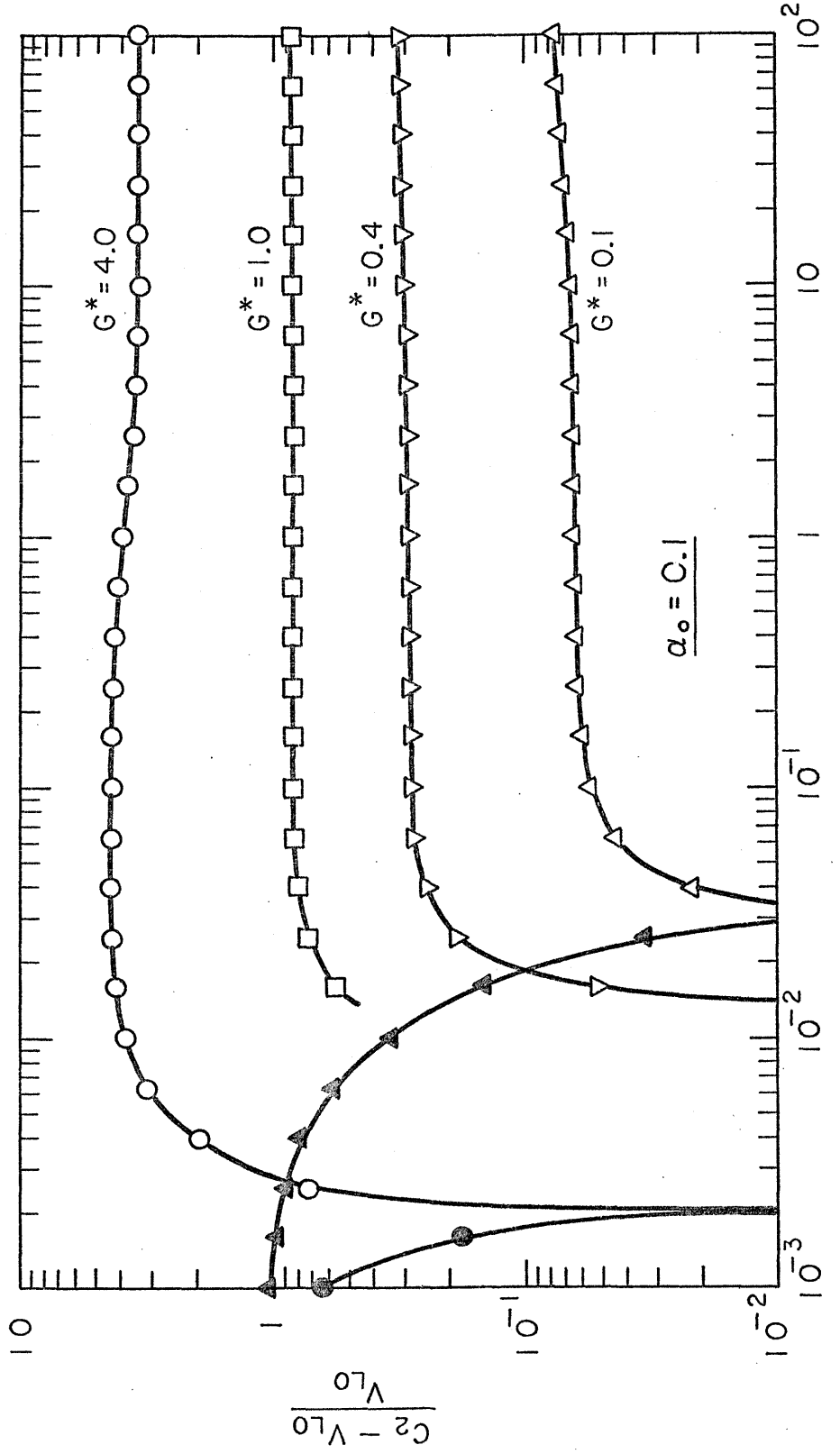

Figure 17. Non-dimensional second kinematic wave speed as a function of reduced frequency $\Omega_c/C_D G$ in the high relative motion Reynolds number flow regime.

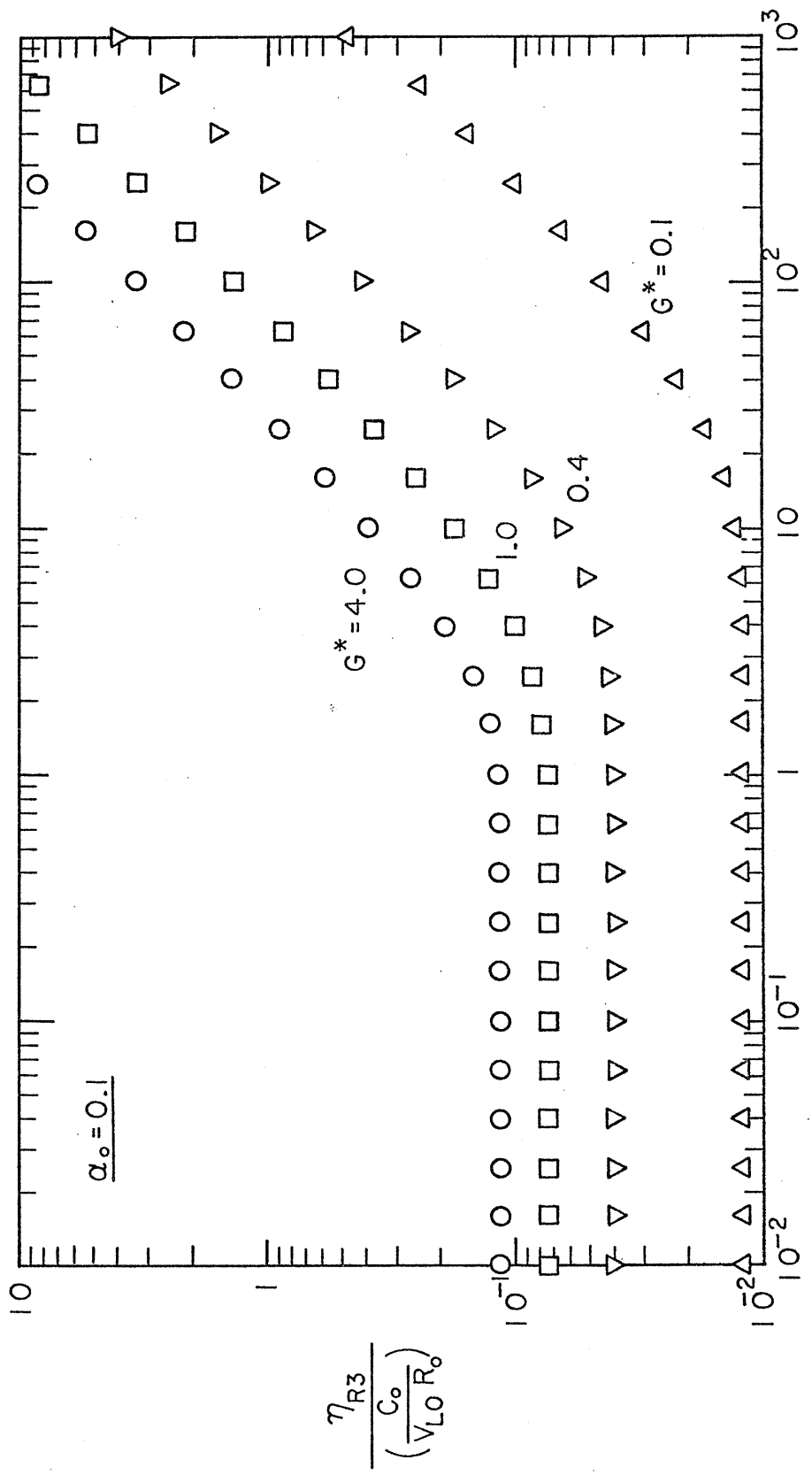

Figure 18. Non-dimensional attenuation of second kinematic wave as a function of reduced frequency Ω_c/C_DG in the high relative motion Reynolds number flow regime.

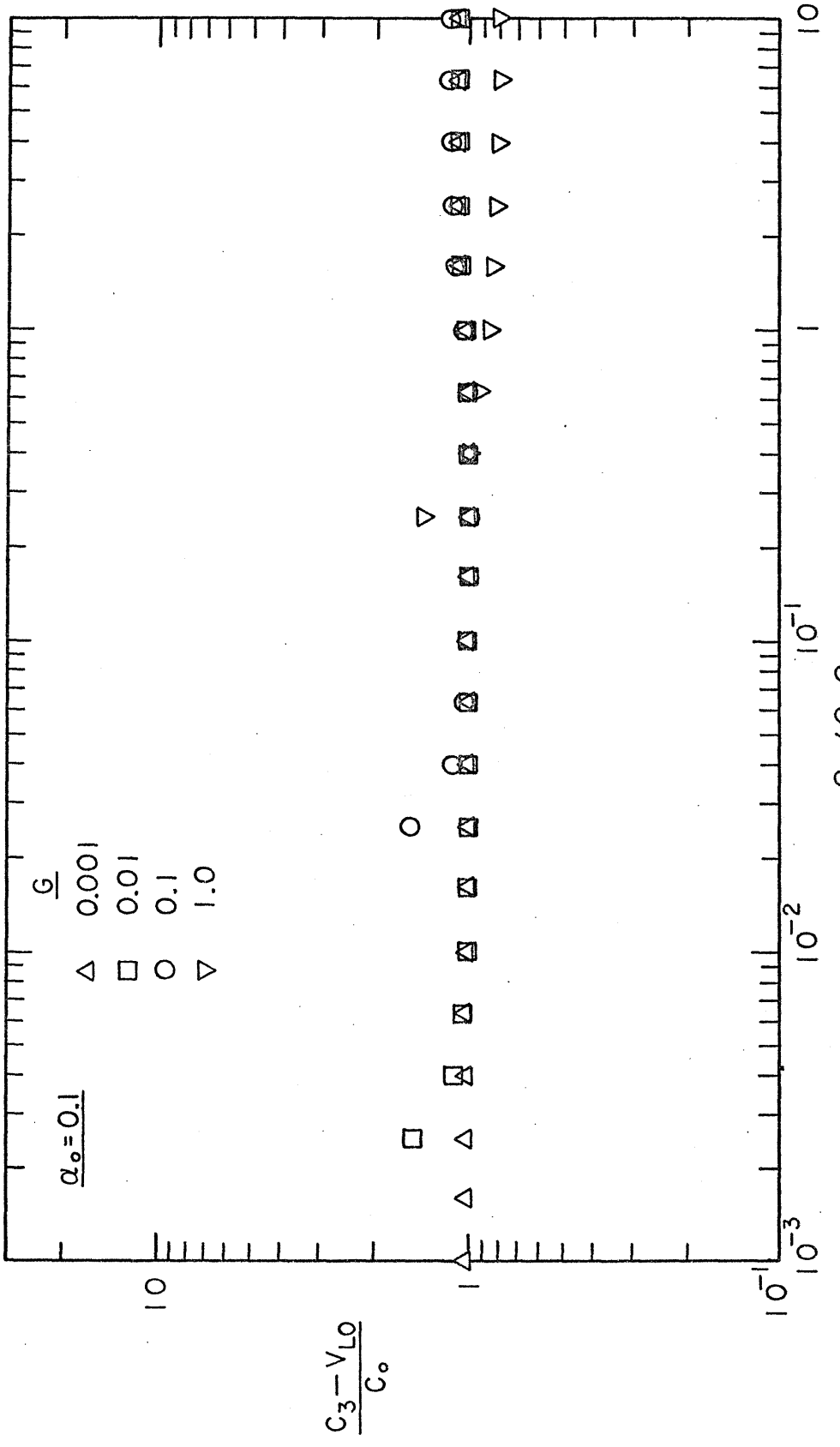

Figure 19. Non-dimensional downstream dynamic wave speed as a function of reduced frequency $\Omega_c/C_D G$ in the high relative motion Reynolds number flow regime.

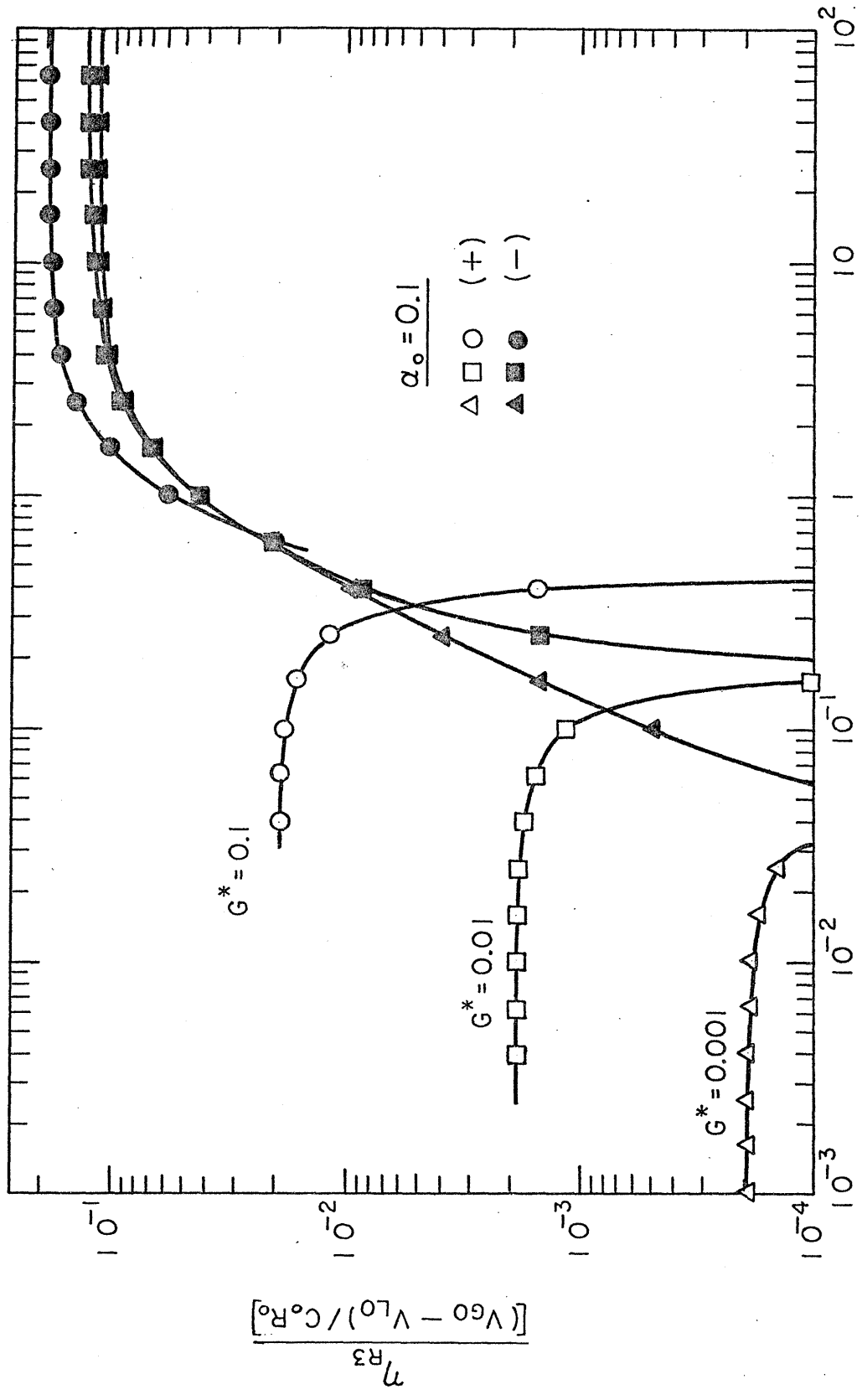

Figure 20. Non-dimensional attenuation of downstream dynamic wave as a function of reduced frequency $\Omega_c/C_D G$ in the high relative motion Reynolds number flow regime.

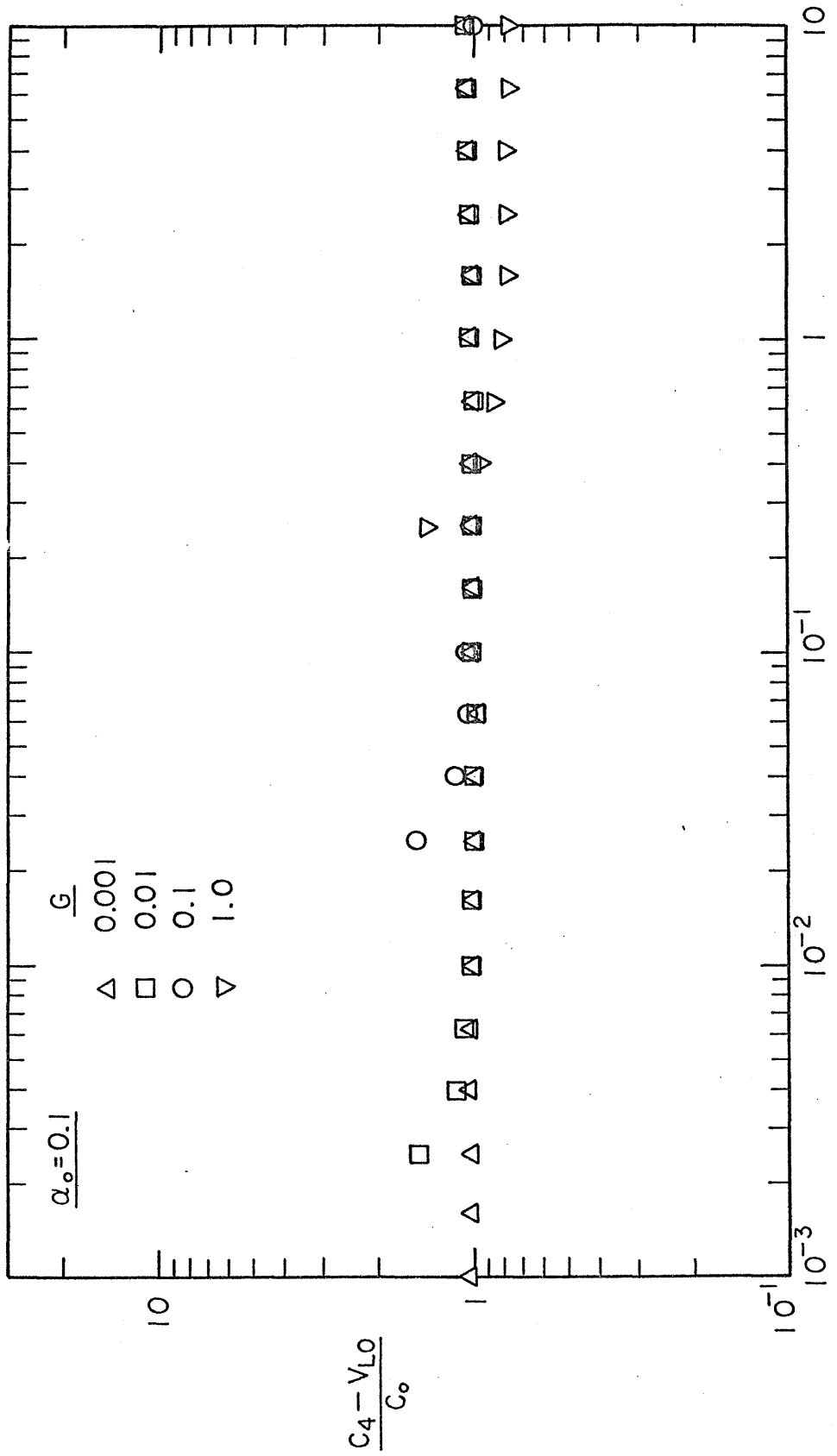

Figure 21. Non-dimensional upstream dynamic wave speed as a function of reduced frequency $\Omega_c/C_D G$ in the high relative motion Reynolds number flow regime.

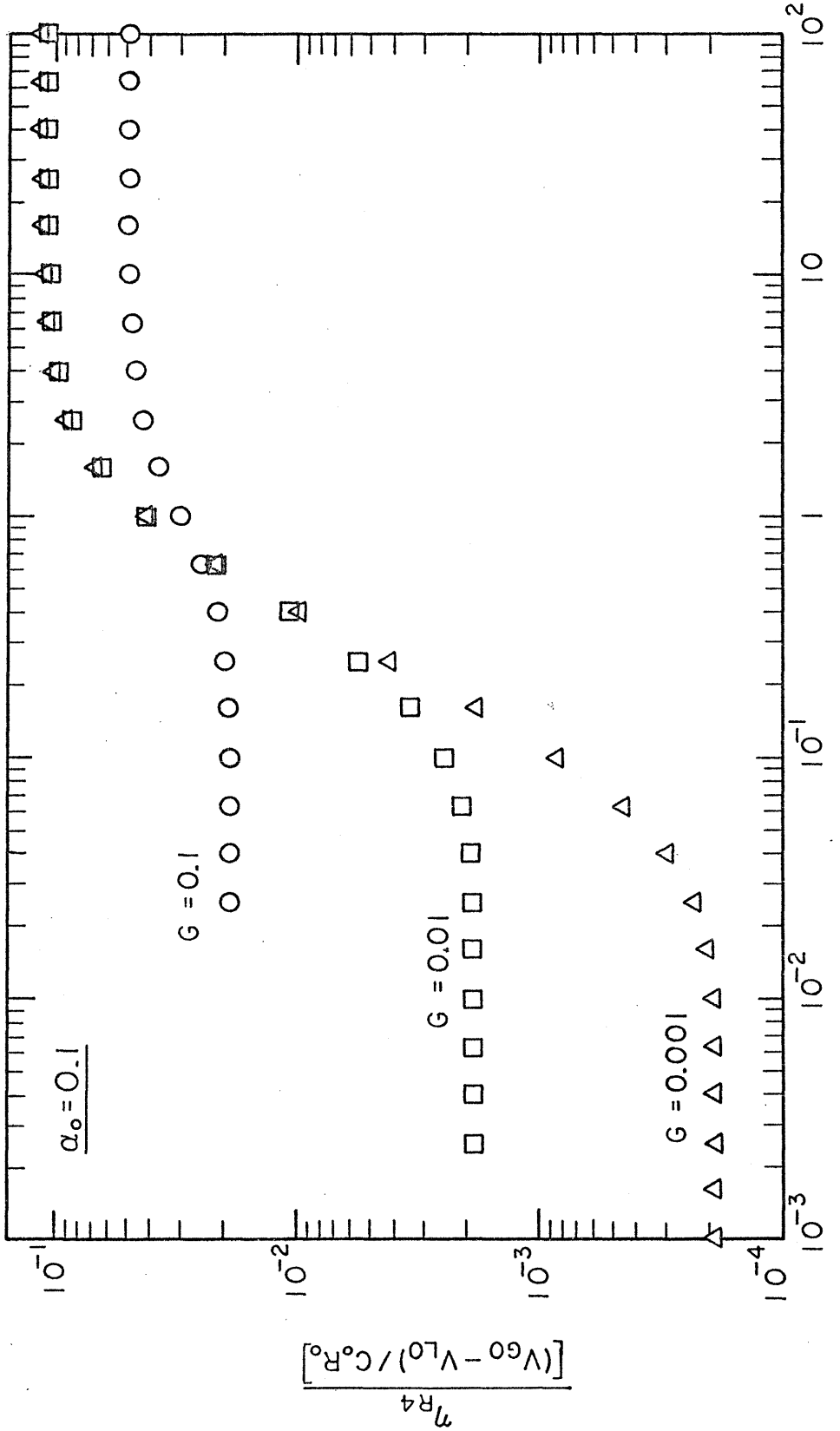

Figure 22. Non-dimensional attenuation of upstream dynamic wave as a function of reduced frequency $\Omega_c/C_D G$ in the high relative motion Reynolds number flow regime.

V. CONCLUDING REMARKS

In this paper, both kinematic and dynamic wave characteristics in various relative velocity and frequency regimes were studied simultaneously by using one simple non-homogeneous model such that the interacting of the waves corresponding to oscillatory perturbations of frequency Ω can be observed. We shall now explore the regimes of validity for a number of wave propagation models which have been extensively used in the past.

Concentrating first on kinematic wave propagation, we shall examine the limits of validity of the drift-flux model [5]. In the drift-flux model, which is basically a kinematic wave model, attention is focused on the relative motion between phases. It is particularly useful if the relative motion is independent of flow rate of each phase. From the continuity equations, the drift-flux model is based on flow properties defined as:

$$\text{volumetric flux} = j = (1 - \alpha_o)V_{Lo} + \alpha_o V_{Lo}$$

$$\text{drift flux} = j_{GL} = \alpha_o(1 - \alpha_o)V_{GL} = \alpha_o(1 - \alpha_o)(V_{Go} - V_{Lo})$$

$$\text{and kinematic wave speed} \quad C = j + \frac{\partial j_{GL}}{\partial \alpha_o}$$

Hence

$$\frac{C - V_{Lo}}{V_{Lo}} = (1 - \alpha_o)\left(\frac{V_{GL}}{V_{Lo}}\right)$$

$$= (1 - \alpha_o)G^*$$

Comparing expression (45) from drift-flux model with the expressions for kinematic wave speeds presented in Tables 5 and 9, it can be seen that the drift-flux model result is limited to the low relative velocity and low frequency regime ($G << \Omega^* << 1$) for low relative motion Reynolds number and ($G << \frac{\Omega_c}{C_D G} << 1$) for high relative motion Reynolds number flow. It can be observed from equation (7) that the drag force is dominant over the added mass (inertia) effect for the above low relative velocity and frequency regimes. The assumption that the relative motion is dominant is therefore satisfied in these regimes and one would expect the drift-flow model to be valid. On the other hand, when the frequency parameter Ω^* or $\Omega_c/C_D G$ is much larger than unity and the relative motion parameter G is much smaller than unity, the kinematic wave speed is given by: (see Table 3 and 7)

$$\frac{C - V_{Lo}}{V_{Lo}} = (1 + \alpha_o)G^* \left[\frac{1 + G^*}{G^*(1 - \alpha_o) + (1 - 2\alpha_o)}\right] \qquad (46)$$

The drift-flux model result has been modified by the expression in the square brackets, hence it only yields the correct wave speed in this flow and frequency regime in the limit as $\alpha_o \to 0$ and/or $G^* = 3$. Obviously, at $\alpha_o = 0$, the result is of little significance. And from equation (46), it can be seen that at $G^* = 3$, the relative motion and inertia effects cancel each other and the last term of expression (46) then disappears, yielding the same result as the drift-flux model.

Turning now to the dynamic wave propagation, let us examine the limits of validity of the conventional homogeneous acoustic model for the propagation of dynamic waves [6]. In this analysis, continuity and

momentum equations are taken into consideration. The relative motion equation is neglected. Based on the zero mass transfer and zero relative velocity assumptions, the acoustic wave model would result in dynamic wave speeds given by

$$C = V_{Lo} \pm \sqrt{\frac{kP_o}{\alpha_o(1 - \alpha_o)\rho_{Lo}}} \tag{47}$$

Since this corresponds to the zero relative velocity case (i.e., $G = 0$), the solution presented in equation (47) is restricted to zero relative motion Reynolds number regime. Examining Table 2, expression (47) for the dynamic wave speeds is valid only at a frequency of oscillation such that Ω^* is much smaller than unity.

On the other hand, at high frequency and zero relative motion, it was shown from Table 1 that the dynamic wave speeds become

$$C = V_{Lo} \pm \sqrt{\frac{kP_o(1 + 2\alpha_o)}{\alpha_o(1 - \alpha_o)\rho_{Lo}}} \tag{48}$$

The factor $\sqrt{1 + 2\alpha_o}$ originates in the inertial effect which dominates the flow at high frequency. This result for the dynamic wave speeds was found by Crespo (1969) (see also Van Wijngaarden [7]) who considered the case where relative motion is not restricted by friction. The concentration of bubbles is then locally less than it is when the bubbles move with the fluid. This gives the mixture a greater stiffness and consequently an acoustic speed larger than $C_o = \sqrt{kP_o/\alpha_o(1 - \alpha_o)\rho_{Lo}}$.

In the high frequency regime, when relative velocity exists ($G \neq 0$), the magnitude of dynamic wave speed is directly proportional

to relative velocity parameter G (see Tables 3 and 7). But as G becomes much larger than unity, the dynamic wave speeds approach values which are solely functions of the void fraction and liquid velocity:

$$C = V_{Lo} \pm C_o\sqrt{\frac{1 - \alpha_o}{2}}$$

They are, in fact, independent of relative velocity.

As mentioned before, since the frequency parameter $\Omega_c/C_D G$ is usually of the order of 10^2 for most engineering bubbly two-phase flow of concern, application of drift-flux and acoustic wave models must be applied with caution. Inertial effects should be included in some cases in order to achieve better accuracy in the prediction of the wave characteristics.

VI. REFERENCES

1. Symington, W.A., 1978, "Analytical Studies of Steady and Non-Steady Motions of a Bubbly Fluid", Ph.D. Thesis, Division of Engineering and Applied Science, California Institute of Technology.

2. Batchelor, G.K., 1967, An Introduction to Fluid Dynamics, Cambridge University Press, p. 233, p. 341.

3. Basset, A.B., 1961, Hydrodynamics, Dover Publications, Inc., New York, p. 270.

4. Landau, L.D. and Lifshitz, E.M., 1959, Fluid Mechanics, Addison-Wesley Publishing Co.

5. Wallis, G.B., 1967, One-Dimensional Two-Phase Flow, McGraw Hill Book Co., p. 89.

6. Hsu, Y.Y. and Graham, R.W., 1976, Transport Process in Boiling and Two-Phase System, Hemisphere Publishing Corp. and McGraw Hill Book Co., p. 101, p. 131.

7. Noordzij, L. and Wijngaarden, L.V., 1974, "Relaxation Effects, Caused by Relative Motion on Shock Waves in Gas-Bubble/Liquid Mixtures", Journal of Fluid Mechanics, Vol. 66, Part 1, p. 115-143.

8. Lighthill, M.J. and Whitham, G.B., 1955, "On Kinematic Waves, I-Flood Movement in Long Rivers", Proceedings of the Royal Society, Vol. 229, p. 281-316.

9. Lighthill, M.J. and Whitham, G.B., 1955, "On Kinematic Waves, II-A Theory of Traffic Flow on Long Crowded Roads", Proceedings of the Royal Society, Vol. 6, p. 317-347.

10. Kinch, G.J., 1952, "A Theory of Sedimentation", Trans. Faraday Society, Vol. 48, p. 166-176.

11. Zuber, N., 1964, "On the Disperse Two-Phase Flows in Laminar Flow Regime", Chemical Engineering Sciences, Vol. 19, p. 897-917.

12. Wallis, G.B., 1962, "A Simplified One-Dimensional Representation of Two Component Vertical Flow and Its Application to Batch Sedimentation", Proc. Symp. on Interaction Between Fluid and Particles, Inst. of Chem. Engrs., London.

13. Gouse, S.W., Jr. and Evans, R.G., 1967, "Acoustic Velocity in Two-Phase Flow", Symp. on Two-Phase Flow Dynamics, Eindhoven, The Netherlands.

14. Moody, F.J., 1968, "The Pressure Pulse Model for Two-Phase Critical Flow and Sonic Velocity", G.E. Rept. No. APED-5579.

15. Bouré, J.A., 1974, "Oscillatory Two-Phase Flows", Von Karman Inst. for Fluid Dynamics, Belgium.

16. Yadigaroglu, G., 1980, "Two-Phase Pipe Flow Instabilities", Von Karman Inst. of Fluid Dynamics, Belgium.